American Heart Journal Plus: Cardiology Research and Practice 42 (2024) 100400

Contents lists available at ScienceDirect

American Heart Journal Plus: Cardiology Research and Practice

journal homepage: www.sciencedirect.com/journal/american-heart-journal-plus-cardiology-research-and-practice

Research paper

Multi-modality imaging for assessment of the microcirculation in peripheral artery disease: Bench to clinical practice

Santiago Callegari [a,b], Attila Feher [a,c], Kim G. Smolderen [b,d], Carlos Mena-Hurtado [a,b], Albert J. Sinusas [a,c,e,*]

[a] Section of Cardiovascular Medicine, Department of Internal Medicine, Yale University School of Medicine, USA
[b] Vascular Medicine Outcomes Program, Yale University, New Haven, CT, USA
[c] Department of Radiology and Biomedical Imaging, Yale University School of Medicine, New Haven, CT, USA
[d] Department of Psychiatry, Yale School of Medicine, New Haven, CT, USA
[e] Department of Biomedical Engineering, Yale University, New Haven, CT, USA

A B S T R A C T

Peripheral artery disease (PAD) is a highly prevalent disorder with a high risk of mortality and amputation despite the introduction of novel medical and procedural treatments. Microvascular disease (MVD) is common among patients with PAD, and despite the established role as a predictor of amputations and mortality, MVD is not routinely assessed as part of current standard practice. Recent pre-clinical and clinical perfusion and molecular imaging studies have confirmed the important role of MVD in the pathogenesis and outcomes of PAD. The recent advancements in the imaging of the peripheral microcirculation could lead to a better understanding of the pathophysiology of PAD, and result in improved risk stratification, and our evaluation of response to therapies. In this review, we will discuss the current understanding of the anatomy and physiology of peripheral microcirculation, and the role of imaging for assessment of perfusion in PAD, and the latest advancements in molecular imaging. By highlighting the latest advancements in multi-modality imaging of the peripheral microcirculation, we aim to underscore the most promising imaging approaches and highlight potential research opportunities, with the goal of translating these approaches for improved and personalized management of PAD in the future.

1. Introduction

Peripheral artery disease (PAD) exerts a significant impact on patient outcomes and burden to the entire healthcare system. PAD carries a global prevalence of 5.6 %, affecting over 230 million patients and over 8.5 million patients in the United States alone [1,2]. The burden of the disease is increasing and shifting to low-to-middle-income countries, with a rise of 28.7 % in the prevalence of PAD in only 10 years [2–5]. On an individual level, the impact of PAD is substantial, ranging from asymptomatic to early-stage claudication (Rutherford 1–3), and ultimately progressing to severe ischemia with rest pain and tissue loss (Rutherford 4–6, termed Chronic Limb Threatening Ischemia). PAD confers a higher risk of long-term cardiovascular mortality than those with myocardial infarction [6]. In addition, PAD is associated with a significant deterioration in functional status and increases the risk of major amputation by 13.9-fold [7,8], with up to 1 in 3 patients with critical limb-threatening ischemia (CLTI) ultimately undergoing amputation [9–11]. Beyond adverse cardiovascular outcomes, PAD is associated with an increased mental health burden and reduced quality of life [10,12–15].

Numerous challenges persist in the management of patients with PAD, and amputation and mortality rates remain high even with current guideline-recommended interventions [16]. Amputations still occur despite successful surgical or endovascular revascularization, even in the absence of infection and patent bypass grafts [16–18]. Patients undergoing a successful endovascular revascularization on adequate guideline-directed medical therapy, still face frequent major amputations (13.2 % at 2 years) [19]. Moreover, amputation rates have risen over the past decade, despite more than doubling the number of endovascular revascularization procedures during the same period [8,20,21].

One of the possible explanations for poor outcomes in spite of adequate revascularization is the presence of unaddressed microvascular disease (MVD), which is an independent predictor of major amputation independent of ankle-brachial index (ABI), diabetes, or PAD disease status [16]. Moreover, MVD plays a synergistic and independent role, rather than a simple additive effect, with a 3.7-fold increase in the risk of major amputation when present, and up to 22.7-fold increase with concomitant PAD (compared to 13.9-fold with isolated PAD) [16].

* Corresponding author at: Section of Cardiovascular Medicine, Department of Internal Medicine, Yale School of Medicine, P.O. Box 208017, DANA 3, New Haven, CT 06520-8017, USA.
E-mail address: albert.sinusas@yale.edu (A.J. Sinusas).

https://doi.org/10.1016/j.ahjo.2024.100400
Received 6 December 2023; Accepted 7 May 2024
Available online 8 May 2024
2666-6022/© 2024 Published by Elsevier Inc. This is an open access article under the CC BY-NC-ND license (http://creativecommons.org/licenses/by-nc-nd/4.0/).

Despite these poor outcomes, current treatments remain primarily focused on the revascularization of the major arteries rather than addressing co-existing abnormalities of the microcirculation [7]. ABI does not assess the microcirculation, and ABIs do not correlate with the degree of MVD [22,23]. In terms of imaging, duplex Doppler and computed tomography (CT) angiography are frequently used to assess PAD anatomy and severity, and while these approaches offer a reasonable assessment of large vessel anatomy, they do not assess microcirculation under standard protocols [24,25].

Developing a deeper understanding of the role of microcirculation using novel imaging modalities could lay the foundation for advancing the evaluation and treatment of MVD. This review will focus on (1) describing the fundamentals of microcirculation structure and function under normal physiological conditions and in the setting of PAD, and (2) outlining current imaging modalities for the assessment of microcirculation in terms of perfusion and molecular imaging, and current gaps in our knowledge (Fig. 1).

2. Microcirculation in skeletal muscle

Given the broad and diverse role of skeletal muscle, the microcirculation within the skeletal muscles is uniquely adaptive [26]. Microcirculation includes vessels with a diameter of <150–200 μm [27]. During strenuous exercise, muscle tissue metabolism increases 20-fold, the intramuscular oxygen consumption and local blood flow 30-fold, and the ATP turnover rate and tricarboxylic acid cycle flux up to a 100-fold [26,28–31]. Moreover, skeletal muscle is a key mediator of central endocrinology hormones, and accounts for 80 % of post-prandial glucose disposal [32–34].

In addition to the dynamic metabolic demands, there is substantial heterogeneity within the muscle fibers. Muscles are composed mainly of type I and type II myofibers, with the composition varying depending on the specific muscle and function [35]. Type I and type II myofibers have varying metabolic energy demands and are affected differently by diseases such as PAD and MVD [35–38]. Type I muscle fibers possess microvessels that penetrate deeper into the sarcolemma and harbor more perivascular mitochondria [39]. Conversely, type II muscle fibers heavily rely on glycolysis, with smaller punctuate and short mitochondrial domains [36]. Denervation of type II fibers due to PAD, and then reinnervation by a different low-motor neuron, converts the type II to a type I myofiber leading to what is called "grouping" [35]. Grouped myofibers have shown to be frequent in patients with PAD [35], likely explaining the extreme variability seen in the type I muscle fiber composition in this population (9–81 %) [40]. The different innervation subsequently changes the metabolism and function of the myofiber. This highlights the complexity of muscle metabolism and the closely intertwined connections between innervation, and circulatory and motor systems.

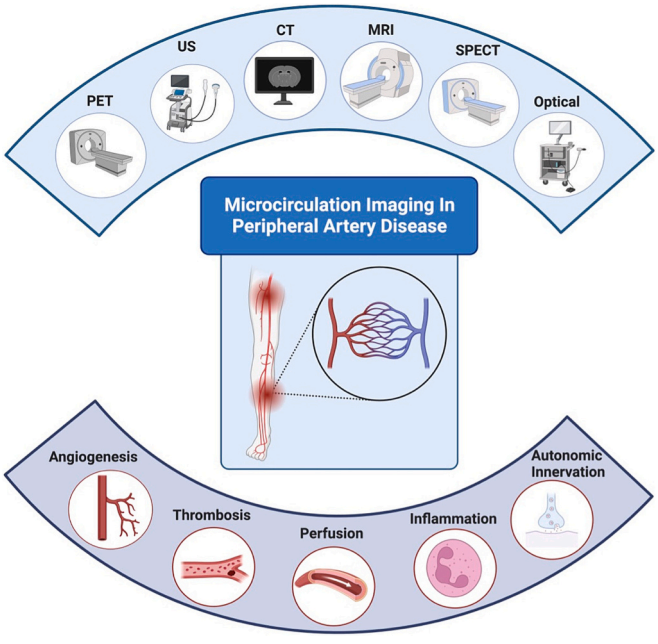

Fig. 1. Imaging Modalities and Targets Evaluated in Evaluating Microcirculation and Microvascular Disease in Peripheral Artery Disease.

Numerous physiological and anatomical abnormalities in the microcirculation are commonly seen in PAD. In patients with CLTI, microvessels have been observed to display wall thinning and impaired vasomotor responses to acetylcholine, nitroprusside, adenosine, and bradykinin [41–43]. Compromised dynamic vascular reactivity in PAD patients is also supported by reduced plasma nitrite levels in responses to exercise [44]. At the histologic level, thickening of the capillary basement membrane and increased volume of the microvessels basement membrane has been shown in PAD, with up to 50-fold higher than healthy controls [45–47]. Capillary density in relationship to PAD has been controversial, with some studies reporting reduced [48–50] and some higher capillary densities [35,51,52]. A few studies have also correlated a lower capillary density with the onset of claudication symptoms and lower oxygen consumption at peak exercise [51–53], while some studies revealed no association of a higher capillary density with improved functional performance [35,40]. Thus, the impact of PAD in the microcirculation anatomy is only beginning to be understood.

Evaluation of reactive hyperemia in response to transient ischemia is one of the most common approaches for assessing the dynamic response of the vasculature in PAD. Reactive hyperemia constitutes a fundamental vascular response that accelerates oxygen delivery to tissues after ischemia, and impaired reactive hyperemia is a marker of elevated cardiovascular risk [54–57]. This response depends on the production of adenosine, endothelium-dependent, and non-endothelium-dependent vasodilators [54]. Peak brachial artery hyperemic flow velocity after a 5-min cuff occlusion of the arm correlates inversely with traditional cardiovascular disease risk factors and markers of inflammation [55,58]. In the context of PAD, reactive hyperemia is blunted due to several mechanisms involving endothelial and nonendothelial-mediated factors [58–60]. However, the exact mechanism leading to the abnormal response of reactive hyperemia and MVD in PAD remains to be fully explored.

3. Perfusion Imaging of the Microcirculation in PAD

Perfusion imaging can evaluate macrovascular and microvascular flow depending on the imaging modality. However, because perfusion is determined significantly by the microcirculation response, we will include all perfusion studies regardless of whether they specify microcirculation imaging, as an assessment of perfusion could be an entry point for understanding MVD (Table 1).

3.1. Ultrasound

Contrast-enhanced ultrasound (CEUS) was introduced in 2005 when it was able to detect differences in time to peak intensity (duration of maximum contrast perfusion) in control versus PAD patients at rest and during exercise [61,62]. Meneses et al. had similar results when using reactive hyperemia and submaximal leg exercise in healthy controls and PAD patients [63]. The authors assessed whole leg and microvascular blood flow during and following 5-min thigh-cuff occlusion, and following a 5-min bout of intermittent isometric plantar-flexion exercise. Whole leg blood flow was assessed as the change in limb volume over the first cardiac cycle from the onset of the 3-s relaxation phase and monitored using an electrocardiogram, heart rate, and beat-by-beat finger blood pressure [64]. Patients with PAD had reduced whole-leg blood flow and lower microvascular perfusion compared to controls

Table 1
Imaging Modalities to Evaluate Perfusion in Microcirculation and Peripheral Artery Disease (PAD), the Main Considerations, and Representative Example in Each Imaging Approach.

Imaging Modality	Advantages	Disadvantages	Employed in PAD and Clinical or Preclinical Stage	Examples
Ultrasound	• Widely and easily available tool in almost all clinical settings. • Variety of protocols available. • Microbubbles greatly enhance the capabilities of conventional ultrasound.	• Observer-dependent technique. • Lacks the level of anatomical detail of other modalities. • No whole-body imaging of the cardiovascular structures.	Yes/Clinical	65, 66
MRI	• Different sequences are available, some requiring contrast or not. • Detailed assessment of soft-tissue structures and better assessment of muscle structures. • BOLD, ASL, and IVIM sequences have been used to assess perfusion in PAD.	• Less available than other techniques. • Longer imaging times compared to other modalities.	Yes/Clinical	81, 84, 98
CT	• Widely available • Whole body imaging and detailed assessment of the structures • Early studies have shown strong correlation with post-revascularization measurements in PAD and CLTI. • Dual Energy CT greatly enhances the capabilities for defining atherosclerotic plaques.	• Has not been vastly employed for perfusion assessment in PAD.	Yes/Clinical	107–109
SPECT	• Combined SPECT/CT protocol evaluated in CLTI correlated with ABI and was predictor of amputation outcomes at 3- and 12-month follow-up. • Widely available nuclear imaging and less costly than PET imaging.	• Less sensitive than PET for image acquisition. • Occasional equivocal study results.	Yes/Clinical	119, 120, 129
PET	• Improved image quality offering higher diagnostic accuracy and interpretability. • Lower dosimetry than SPECT imaging • [^{15}O] water, [^{13}N] ammonia, [^{82}Rb] perfusion imaging has been successfully used to quantify perfusion.	• Not widely available • Higher costs	Yes/Clinical	126, 127

Abbreviations: PAD, Peripheral Artery Disease; MVD, Microvascular Disease; MRI, Magnetic Resonance Imaging; BOLD, Blood-oxygen-level-dependent Imaging; ASL, Arterial Spin Labeling; IVIM, Intravoxel Incoherent Motion; CT, Computerized Tomography; CLTI, Chronic Limb-threatening Ischemia; SPECT, Single Photon Emission Computed Tomography; PET, Positron Emission Tomography; CLTI, Chronic Limb-threatening Ischemia; ABI, Ankle-brachial Index.

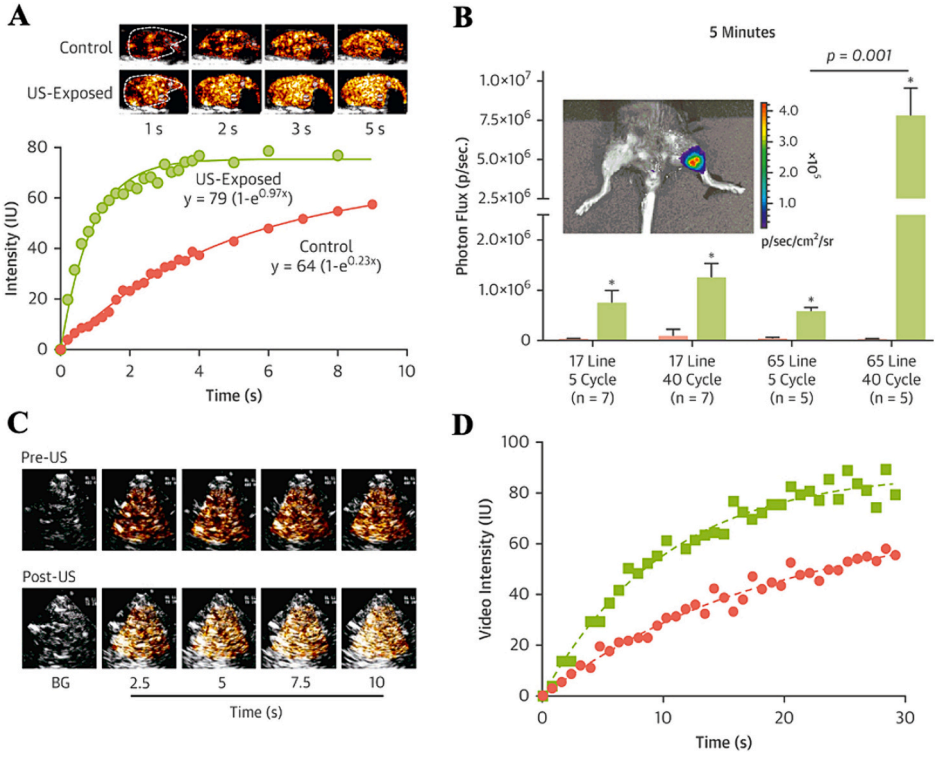

Fig. 2. Lipid-shelled Decafluorobutane Microbubbles for Contrast-Enhanced Ultrasound (CEUS) Is a Promising Area for Perfusion Assessment, Microvascular Disease Evaluation, and Therapeutics. The Study by O'Neil et al. Evaluated the Use of Microbubbles for Cavitation And Improve Blood Flow in the Microcirculation. The Authors Applied the Microbubbles In Mice to Enhance Perfusion Compared to the Contralateral Control Leg (Fig. A & B), Denoting an Increased In the Intensity (Fig. A) and Photon Flux (Fig. B) When Evaluting Optical Imaging of Adenosine Triphosphate After the CEUS. This Method Was Also Employed in Humans, Denoting an Increased Perfusion in the US Images (Fig. C) and Intensity (Fig. D), Given by an Increase in Flow Attributed to the Flux Rate and Microvascular Blood Volume (Plateau Intensity) Comparing Before (Orange) and After US (Green). *Figure adapted from O'Neil J Am Coll Cardiol Img. 2020 Mar, 13 (3) 641–651.* (For interpretation of the references to colour in this figure legend, the reader is referred to the web version of this article.)

[63]. However, different results were observed during submaximal exercise, with no difference between the groups regarding arterial blood flow, but higher microvascular flow in patients with PAD, confirming the reduction was determined by the presence of MVD [63]. Another study found similar results and confirmed restoration of the microcirculation changes after successful revascularization [65]. In addition, a study by Mason et al. optimized a protocol for using CEUS in mice and translated the protocol to healthy controls and patients with PAD, while also exploring the potential role of microbubble cavitation in increasing regional flow (Fig. 2) [66].

Another approach for the assessment of microcirculation is laser Doppler imaging, which has been used to assess endothelial function in PAD [67,68]. Muzaffer et al. used this method to evaluate vascular reactivity in response to exposure to acetylcholine and sodium nitroprusside in patients with PAD due to atherosclerosis or Buerger's disease [68]. Vasodilation responses were reduced in patients with PAD following infusion of these mediators, and plasma nitric oxide was consistently higher in PAD patients and correlated with microvascular flow, blood glucose, and HbA1c in 114 patients. Similar methodologies also explored the role of these vasodilators and found consistent results using laser-Doppler fluxmetry [67].

3.2. Optical imaging

Near-infrared spectroscopy (NIRS) is a noninvasive method that involves delivering light with a wavelength between 630 and 830 nm, and using a diffusion-based model to calculate multiple metrics such as recovery time, deoxygenation, oxygen consumption and saturation, and hemoglobin parameters [69–71]. Individual studies have validated the use of NIRS to screen potential patients with PAD or for oxygen-guided exercise regimens [70–72]. One of the most robust parameters of NIRS is the oxyhemoglobin area under the curve, which has been recommended as the measurement parameter for assessment and follow-up of PAD [70]. However, extensive heterogeneity between studies and parameters evaluated has limited the widespread adoption of the technology [70,71,73]. Spatial frequency domain imaging and hyperspectral imaging have also been shown to detect microcirculation differences in PAD and healthy controls in smaller studies [74–80].

3.3. Magnetic resonance imaging

Blood oxygen level-dependent (BOLD) MRI has been used to assess tissue oxygenation in specific muscles with high reproducibility, especially the maximum hyperemic peak value and minimum ischemic value [81–84]. Originally developed for neuroimaging studies, BOLD sequences rely on the magnetic susceptibility difference between paramagnetic deoxyhemoglobin and diamagnetic oxyhemoglobin [85]. BOLD MRI has been used to assess blood flow and ischemia, as well as for diagnosis and evaluation of PAD revascularization [82,85,86]. When assessing reactive hyperemia in response to a 6 min cuff compression, reduced peak hyperemic values (HPV) and delayed time to peak (TTP) were seen in patients with symptomatic PAD and correlated with ABI [86]. A trend to normalization of TTP and HPV has also been documented after successful revascularization procedures [87].

Arterial spin labeling (ASL), intravoxel incoherent motion (IVIM) MRI imaging, and contrast-enhanced MRI modalities have also shown promising results for evaluating MVD [88–91]. With ASL, a control scan is obtained, and then tagged protons in arterial blood are given a magnetic tag, which results in different magnetic properties from the surrounding tissue [91]. Continuous and pulsed ASL have demonstrated reduced peak exercise calf perfusion in PAD [88–90]. On the other hand, IVIM MRI is based on the analysis of the random movement of individual molecules without the need for contrast, similar to diffusion-weighted MRI [92,93]. A few studies have evaluated IVIM for the assessment of the difference in the microcirculation and perfusion in controls with PAD and CLTI, [94,95] observing improvement in the diffusion coefficient D after endovascular procedures. This is in part due to expected inflammation of the blood vessels and muscle tissues after successful revascularization, which leads to increased diffusivity of water molecules within muscles [95,96]. Recently, contrast-enhanced MRI also showed promising results showing a significant correlation of parameters derived from computational modeling such as permeability of the microvasculature, fraction of extracellular space, and microvascular pressure, among others, with ABI, claudication onset time, and peak walking time (Fig. 3) [97].

Suo et al. compared the ability to diagnose and assess the severity of PAD using comprehensive MRI evaluation (BOLD, ASL and IVIM) in young healthy controls, age-matched controls, and 14 patients with PAD [98]. All parameters (ASL-derived blood flow values, BOLD-derived T2* values, and IVIM-derived perfusion fraction (*f*) values) were correlated with transcutaneous oxygen measurements [98]. BOLD imaging parameters provided more robust results and significant correlation with established markers of PAD diagnosis and severity. Interestingly, none of the measurements between the 3 imaging modalities correlated with each other, which also relates to the different mechanisms to derive their metrics: BOLD T2* values are strongly related to tissue oxygenation, IVIM to the pseudo-diffusion of the capillary beds, and ASL to blood delivery into tissues.

T1 mapping was recently introduced as a possible way for assessing skeletal muscle scarring [99,100]. T1 mapping rely on the measurement of the longitudinal or spin-lattice relaxation time, which by itself is determined by how rapidly the protons re-equilibrate their spins after a radiofrequency pulse [101]. Native T1 values are a composite of the signal of myocytes and extracellular volume, and the values can be increased in the setting of edema or fibrosis [101]. A few studies have evaluated the role of T1 mapping in PAD, and demonstrated the potential to evaluate the degree of interstitial muscle fibrosis in skeletal muscle. A positive correlation of native T1 and T1 derived extracellular volume was observed in comparison with functional parameters (6-min walking and 3-min stepping test) in patients with PAD and diabetes [99,100].

3.4. Computerized tomography (CT)

CT is widely used in the evaluation of multiple cardiovascular conditions, although the focus has been mainly on the assessment of coronary blood flow and coronary microcirculation, [102–106] with relatively few studies using CT imaging to assess the peripheral microcirculation [107–109]. Our group applied CT angiography successfully in the measurement of physiologic changes in epicardial vessel diameter in response to dobutamine and adenosine vasoactive responses, and the secondary flow-mediated response associated with microvascular vasodilation [110]. The observed impairment in epicardial vessel dilation associated with a doxorubicin-induced cardiotoxicity was indicative of MVD [110]. Moreover, animal models have shown a good correlation of CT-derived myocardial blood flow (MBF) with microsphere-derived blood flow [102,103]. In human studies, quantification of myocardial perfusion/MBF using CT in comparison with [^{82}Rb] PET perfusion had a <20 % error range [106].

A developing approach that could be implemented to further enhance the capabilities of CT for assessing perfusion and MVD is the use of dual energy CT (DECT) [111–113], which applies two different x-ray beam energies yielding images with greater soft tissue differentiation. Although pioneering work has used DECT in PAD [111,112], more studies are needed to further assess the capabilities of DECT in assessing peripheral MVD.

3.5. Single-photon emission computerized tomography (SPECT) perfusion

SPECT is a promising modality for the assessment of perfusion in PAD. Early SPECT studies using planar ^{99m}Tc-sestamibi indicated a decrease in proximal and distal perfusion in asymptomatic PAD patients

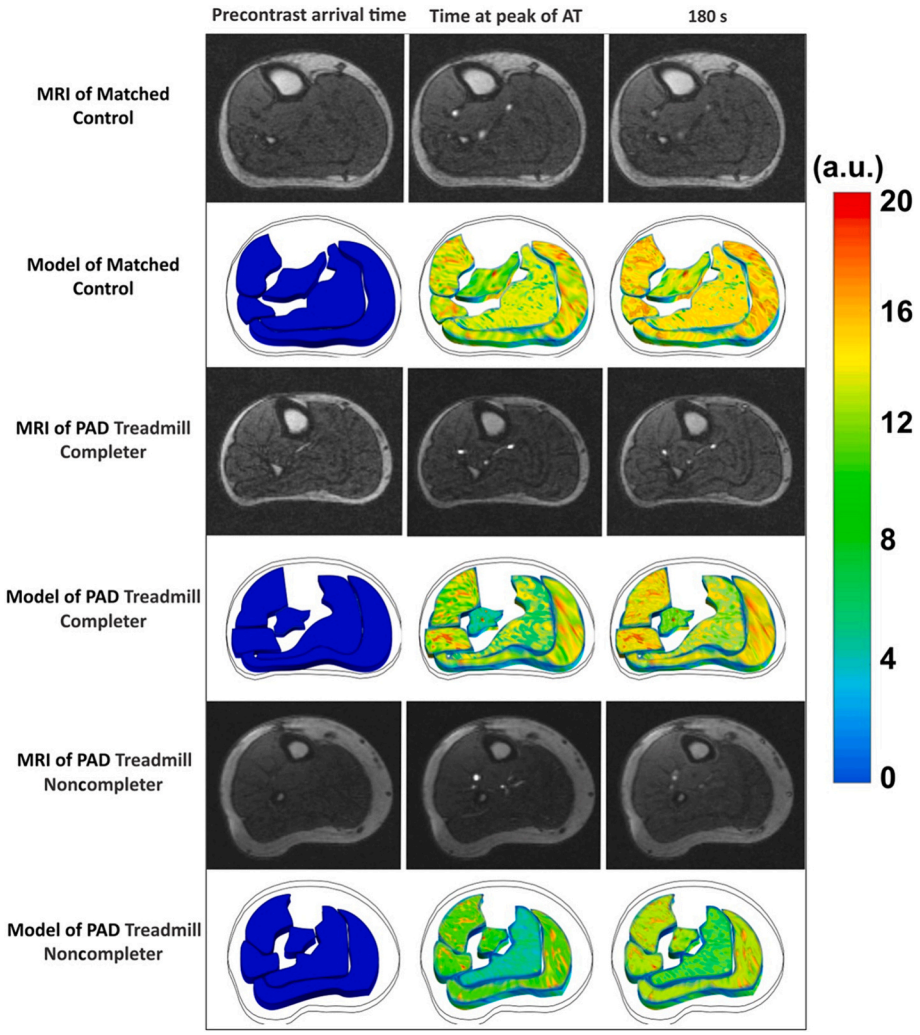

Fig. 3. Contrast-enhanced Magnetic Resonance Imaging (MRI) Has Also Been Used in Microvascular Disease in Peripheral Artery Disease (PAD). Gimnich et al. Applied Contrast-enhanced MRI in 3 Different Types of Patients (Healthy Control, PAD Patient After a Completed 6-min Treadmill Protocol, and PAD Patients Who Were Not Able To Complete The Treadmill Protocol) and Evaluated at 3 Different Time Points (Pre-contrast Arrival Time, Time at the Peak of the Anterior Tibial Artery, and 180 Seconds After). The Images Were Analyzed Using Computational Microvascular Modeling of 5 Distinct Calf Muscle Compartments. The Model Revealed Marked Differences Across the Microvascular Response in the Different Patients, Time Points, and Muscle Compartments. *Figure from Gimnich* et al. *Journal of the American Heart Association. 2023;12:e027649.*

with early-stage atherosclerosis, demonstrating an impairment in both rest and stress perfusion compared to control subjects [114,115]. Subsequent research confirmed that ^{99m}Tc-based radiotracers enable both qualitative and quantitative assessment of lower extremity perfusion. Estimates of perfusion, derived using SPECT imaging, showed significant correlations with angiographic assessments and Doppler findings in patients with PAD and demonstrated changes after revascularization [116–118].

Preclinical studies have explored the utility of SPECT imaging in evaluating MVD in PAD. A combined SPECT/CT protocol was applied to healthy individuals and 42 patients with CLTI and demonstrated that resting perfusion in patients with CLTI was notably lower than in controls, and this difference displayed excellent agreement between serial measurements and strong correlation with ABI [119]. However, in the setting of patients with diabetes, SPECT/CT imaging was not correlated with ABI, likely as a result of the inability of ABI measurements to assess MVD. In a follow-up study, SPECT/CT imaging was related to amputation outcomes in patients with CLTI after endovascular revascularization (Fig. 4) [120]. The patients with a greater improvement in microvascular perfusion had an improved amputation-free survival rate at 3- and 12-month follow-up [120].

3.6. Positron Emission Tomography (PET)

Quantitative PET perfusion imaging has been shown to be highly accurate in animal models and has been translated for clinical application. Perfusion measurements using [^{15}O] water and [^{13}N] ammonia to assess impairment in calf muscle flow reserve among animals and PAD patients exhibited a strong correlation with flow measurements obtained through thermodilution, microsphere-derived values, and Doppler flow probe assessments [121–123]. Penuelas et al. demonstrated a strong correlation between PET-derived blood flow values and those obtained through microsphere analysis in mice, along with a relationship between PET-measured perfusion and histological indicators of tissue fibrosis and necrosis [124]. Clinical studies have also shown changes in perfusion in healthy individuals who underwent exercise training [125]. In addition, among patients with CLTI, a reduced exercise-induced blood flow was noted with [^{15}O]PET imaging [126]. Perfusion imaging using [^{82}Rb] PET demonstrates a strong correlation with [^{15}O] PET-derived perfusion [127].

Each PET tracer has relative advantages and disadvantages and have enabled assessment of perfusion in different settings. Tracers with short half-lives (e.g., [^{13}N] ammonia, [^{15}O] water, [^{82}Rb]) have allowed for

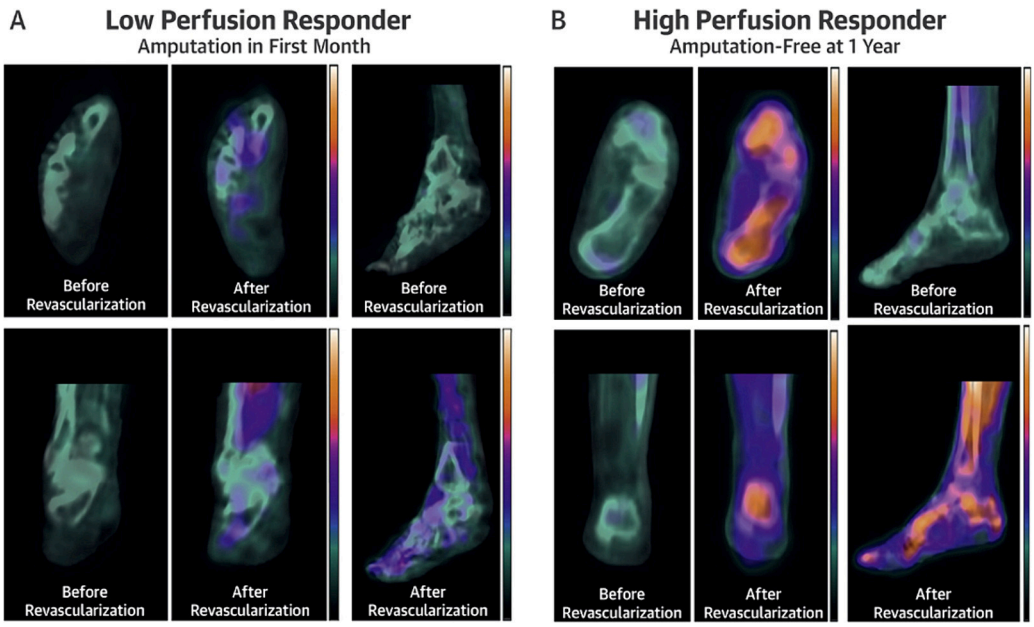

Fig. 4. A Combined SPECT and CT Protocol Evaluated by Chout et al., Has Shown Promising Results as a Potential Modality to Assess Post-Revascularization Outcomes in Patients with Critical Limb-threatening Ischemia (CLTI) and Diabetes. According to the Protocol, a Low-Perfusion Responder (Fig. A) Was Found to Have Lower Amputation-Free Survival at 3 and 12 Months Compared to the High-Perfusion Responder (Fig. B) After Endovascular Revascularization. The Sensitivity and Specificity of the Imaging Were Reported as 78.6 % and 81.8 %, Respectively. *Figure From: Chou, T.H.* et al. *J Am Coll Cardiol Img. 2021;14(8):1614–24.*

multiple measurements on the same patients within a single day. A [^{18}F] labeled perfusion agent like [^{18}F] Flurpiridaz [128], which possesses a longer half-life (~110 min) and high extraction rate, offers the potential for evaluating relative perfusion reserve in the lower extremities during exercise, and even the possibility of performing both cardiac and peripheral imaging following a single radiotracer injection, however at the cost of higher radiation exposure. Our group has been exploring the use of dynamic [^{82}Rb] PET for quantitative perfusion of the lower extremities in patients with PAD for evaluation of microvascular perfusion. [129]

4. Molecular imaging in assessment of the microcirculation in PAD

4.1. Angiogenesis

Angiogenesis represents the formation of new microvessels in response to hypoxia and ischemia. A broad array of ultrasound, SPECT, and PET modalities have been developed for imaging angiogenesis, including targeting endothelial cell proteins, angiogenic factors, cell mediators, and extracellular matrix proteins [130,131] (Table 2 and 3).

One of the most studied targets is the $\alpha_V\beta_3$ integrin. Contrast-enhanced ultrasound (CEUS) with microbubbles directed towards the $\alpha_V\beta_3$ integrin has been extensively studied. Leon-Poi et al. used these microbubbles in a hindlimb ischemic rat model undergoing injections of fibroblast growth factor-2 (FGF-2). Rats treated with the angiogenic factor had a greater rate and extent of blood flow recovery, as well as greater signal from integrin-targeted microbubbles [132]. Xie et al. also successfully evaluated angiogenesis using CEUS targeted to the $\alpha_V\beta_3$ *integrin* for assessing therapeutic mutations of hypoxia-inducible factor 1α (HIF-1α) [133]. In addition to the CEUS imaging, Jo et al. recently developed a novel contrast agent for MRI targeting the $\alpha_V\beta_3$ integrin, which successfully tracked angiogenesis in a mouse model of hind-limb ischemia [134].

Radiotracers have also been used to evaluate angiogenesis in PAD models. Using the [^{99m}Tc]NC100692 radiotracer targeting $\alpha_V\beta_3$ integrin, Hua et al. demonstrated temporal changes of ischemia-induced angiogenesis in a murine hindlimb model after acute femoral occlusion [135], and subsequent studies introduced a semi-quantitative approach to evaluate this methodology [136]. In PET, RGD-based radiotracers such as [^{18}F]Galacto-RGD have demonstrated specific uptake in atherosclerotic lesions of mouse aorta and yield significant potential to evaluate angiogenesis and inflammation in atherosclerotic lesions [137,138].

Related biomarkers such as P-selectin and CX_3CR-1 have also been explored using CEUS. Ryu et al. documented improvement in the recruitment of proangiogenic monocytes and enhanced chemotaxis in mice with iliac artery ligation using multipotential adult progenitor cells (MAPC) [139]. In this study, the expression of P-selectin and CX_3CR-1 was assessed with CEUS and microbubbles targeting P-selectin and CX_3CR-1 [139].

Vascular endothelial growth factor (VEGF) and related proteins have also been a common target in peripheral imaging. Using SPECT imaging of [^{99m}Tc]DOTA-PEG-scVEGF that *targets the VEGF receptor, Tekabe* et al. *found a stronger signal for evaluating angiogenesis compared to another* [^{99m}Tc] radiotracer *targeting the* $\alpha_V\beta_3$ *integrin in* a mice model of limb ischemia using femoral artery ligation [140]. Interestingly, immunofluorescent analysis revealed the uptake of these radiotracers is non-overlapping, and could potentially be used to assess different cell types and processes [140]. PET imaging with [^{64}Cu] labeled radiotracers has also shown increased uptakes with angiogenesis-promoting treatments in animal models [141,142]. Wilmann et al. demonstrated in a mice hindlimb ischemia model an increased uptake of [^{64}Cu]VEGF-121, which also further increased after an exercise intervention [143]. Similar results were seen in a rabbit model using a [^{111}In]labeled recombinant human VEGF-121 at 10 days post femoral ligation [131,144]. Consistent with murine models, Stacy et al. using a porcine animal model of acute femoral artery occlusion and a combined CT and SPECT imaging with a [^{201}Tl] radiotracer, quantify sequential alterations in lower extremity angiogenesis and segmental resting perfusion from baseline to 4-week post occlusion [145].

The complementary role of the diverse imaging modalities was also recently explored by Hedhli et al. using 4 imaging modalities: Power Doppler, laser speckle contrast, photoacoustic imaging, and tandem radio-labeled molecular probes [^{99m}Tc]NC100692 that target angiogenesis and another [^{99m}Tc]BRU-5921) that identifies hypoxia [146]. These authors documented the spectrum of landmarks in vascular

Table 2
Imaging Modalities to Evaluate Molecular Imaging in Microcirculation and Peripheral Artery Disease (PAD), the Main Considerations, and Representative Example in Each Imaging Approach.

Imaging Modality	Main Considerations and Targets	Employed in PAD and Clinical or Preclinical Stage	Examples
Angiogenesis	The $\alpha_V\beta_3$ integrin has been frequently targeted with Contrast-enhanced ultrasound (CEUS), SPECT radiotracers, and pilot studies with MRI contrast agents.	Yes/Clinical	132–134 139
	P-selectin and CX_3CR-1 have also been studied with CEUS.		140–142
	VEGF-related targets have also been explored with SPECT and PET, and seem to be non-overlapping to $\alpha_V\beta_3$ integrin tracers.		
Inflammation	Contrast-enhanced ultrasound neutrophils, α5 integrins, and VCAM-1.	Yes/Preclinical	132,147
	SPECT imaging using labeled compounds with diphosphonate,		148–150
	antigranulocyte antibodies, and indium-111 labeled leukocytes has been used.		153, 160
	PET imaging has also been used to detect early subclinical arterial inflammation and microcalcification.		
Thrombosis	Not explored for MVD or PAD or extensively studied in the clinical setting. Radiotracers are available targeting fibrin and GpIIb/IIIa receptor.	No/Clinical	163–165
Autonomic Innervation	Not extensively explored for MVD or PAD. Radiotracers available targeting norepinephrine transporters.	No/Clinical	176–178

Abbreviations: CEUS, Contrast-enhanced Ultrasound; SPECT, Single Photon Emission Computed Tomography; VEGF, Vascular Endothelial Growth Factor; PET, Positron Emission Tomography; MVD, Microvessel Disease; PAD, Peripheral Artery Disease.

recovery: loss of perfusion and increased hypoxia resulting in nitric oxide release, vascular recovery in subcutaneous tissue, and molecular signatures of angiogenesis in the deep leg tissue [146].

4.2. Inflammation

CEUS imaging has also been used to assess inflammation using targeted microbubbles. Behm et al. used microbubbles targeting neutrophils, α5 integrins, and VCAM-1 in a murine animal model of hind-limb ischemia. CEUS imaging demonstrated early signal enhancement of the 3 targets when blood flow was low (<20 % control blood flow) at day 2 post occlusion. While neutrophil signals declined between day 2–4, VCAM and monocyte microbubble signaling persisted until day 7 [147]. Similarly, SPECT imaging has been evaluated using [^{99m}Tc] labeled compounds with diphosphonate, anti-granulocyte antibodies, and indium-111 labeled leukocytes to assess inflammation [148–152]. Most studies using SPECT to analyze MVD have combined CT protocols to accurately localize targeted radiotracers.

[^{18}F]Fluorodeoxyglucose (FDG) PET imaging has also been used to detect early subclinical arterial inflammation by tracking FDG uptake in inflammatory cells [153,154]. This approach relies on calculating target-to-background ratio (TBR) or computing standardized uptake values (SUVmax) in arteries relative to blood pool's SUVmax [25]. These quantitative measurements have also been strongly correlated with arterial stiffness [155]. Other radiotracers such as [^{68}Ga]pentixafor and [^{11}C]PK11195 targeting specific immune cells [156–159], and could support studies investigating the role of inflammation in the pathogenesis of MVD in PAD. Using [^{18}F]FDG and [^{18}F]sodium fluoride, Reijrink et al. demonstrated a significant correlation between arterial inflammation and microcalcification in diabetic patients [160]. These two radiotracers have also been successfully employed to trace microcalcifications and inflammation in PAD within the context of diabetes, chronic kidney disease, and statin use, with a strong correlation with CT calcified plaque scores and potential for predicting 1-year restenosis after angioplasty (Fig. 5) [160,161]. The use of these radiotracers in the setting of MVD could improve understanding of PAD pathogenesis provide better risk stratification, and enable monitoring of revascularization procedures.

4.3. Thrombosis

As the peripheral microcirculation is highly vulnerable to be

Table 3
Most Promising SPECT and PET Radiotracers To Assess Microcirculation in Peripheral Artery Disease.

SPECT Tracers		Clinical or Preclinical phase	Evaluated in PAD or PAD Model	References
Perfusion	[^{99m}Tc] sestamibi	Clinical	Yes	[114]
	[^{99m}Tc] tetrofosmin	Clinical	Yes	[119,120,179]
	^{201}Tl	Clinical	Yes	[145,115]
Angiogenesis	[^{99m}Tc] NC100692	Preclinical	Yes	[135]
	[^{99m}Tc] DOTA-PEG-scVEGF	Preclinical	Yes	[140]
	[^{99m}Tc] BRU-5921	Preclinical	Yes	[146]
PET Tracers				
Perfusion	[^{13}N] ammonia	Clinical	Yes	[122,123]
	[^{15}O] water	Clinical	Yes	[121–123,126]
	[^{82}Rb]	Clinical	Yes	[127,129]
	[^{18}F] Flurpiridaz	Clinical	No	[128]
Angiogenesis	[^{18}F] Galacto-RGD	Clinical	No	[137,138]
	[^{64}Cu] VEGF-121	Preclinical	Yes	[141–143]
Inflammation	[^{18}F] Fluorodeoxyglucose (FDG)	Clinical	Yes	[153,154]
	[^{68}Ga] Pentixafor	Clinical	Yes	[156]
	[^{11}C] PK11195	Clinical	Yes	[157]
Thrombosis	[^{68}Ga]FBP & [^{111}In]FBP15	Preclinical	No	[163,164]
	[^{18}F] GP1	Clinical	No	[165]
	[^{64}Cu] FBP8	Clinical	No	[166]
Autonomic Innervation	6-[^{18}F] fluorodopamine	Clinical	No	[173]
	[^{11}C] HED	Clinical	No	[175]
	[^{18}F] LMI1195	Clinical	No	[176–178]

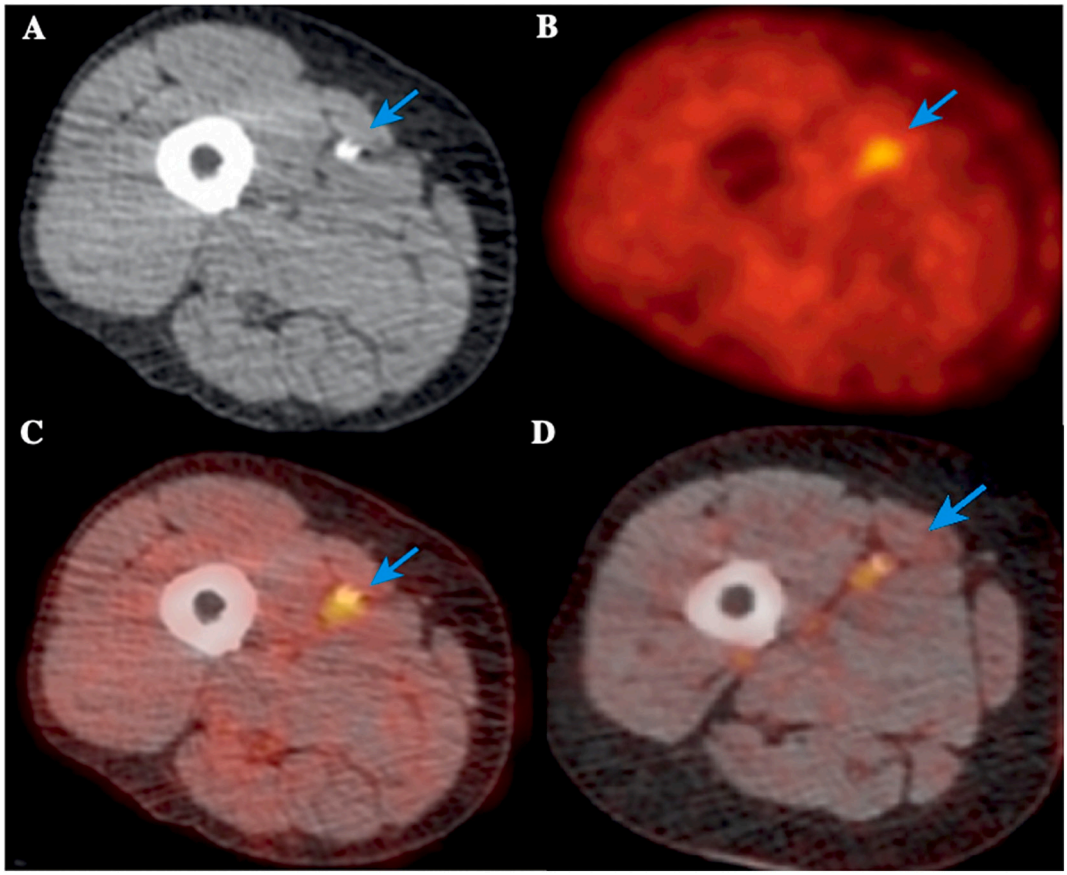

Fig. 5. Early Efforts Have Shown the Potential of PET Imaging to Predict Outcomes in Vascular Disease. Chowdhury et al. Evaluated Patients With Peripheral Artery Disease (PAD) Before and 6 Weeks After Angioplasty. Patients with Signal Uptake (Blue Arrow) Denoted at Baseline in the Non-contrast CT (Fig. A), 18F-FDG PET (Fig. B), and Fused 18F-NaF PET/CT (Fig. C), that Persisted 6 weeks after Angioplasty (Fig. D), Was Significantly Associated with Restenosis of the Vessel at 1-Year. *Figure adapted from Chowdury* et al. *J Am Coll Cardiol Img. 2020 Apr, 13 (4) 1008–1017.* (For interpretation of the references to colour in this figure legend, the reader is referred to the web version of this article.)

occluded or damaged by thrombosis [162], evaluating thrombosis could serve as a potential measure of disease severity related to disruption of the microcirculation. Multiple PET and SPECT radiotracers evaluating thrombus formation have been identified. For example the [^{68}Ga]DOTA-fibrin-binding-probe [^{68}Ga]FBP and [^{111}In]FBP15, which specifically targets fibrin [163], and [^{18}F]GP1 [164] and [^{64}Cu]FBP8 [165,166], which binds to the GPIIb/IIIa receptor involved in platelet aggregation [167]. None of these tracers have been used to specifically assess microcirculation in PAD, but the use of these targeted radiolabeled probes hold significant potential for future preclinical and clinical studies in PAD.

4.4. Autonomics

Sympathetic activity promotes vasoconstriction of the microcirculation, with a wide variety of heterogeneous and regional effects given by differential distribution of α_1 and α_2 receptors in arteriolar smooth muscle, different sensitivity in proximal and distal muscle fibers, among others [168–170]. However, local factors can enable the distal arterioles to "escape" sympathetic effects [168]. [169] Recently, PET imaging of autonomic innervation has emerged as a potential tool to improve risk stratification associated with cardiovascular disease [171,172]. Because of the high heterogeneity of skeletal muscle flow and sympathetic innervation, targeted imaging of sympathetic activity could improve our understanding of the role of autonomic innervation in flow regulation, and serve as a possible predictor of outcomes. Tracers such as 6-[^{18}F] fluorodopamine [173,174], [^{11}C]hydroxyephedrine [175], and [^{18}F] LMI1195 [176–178] could be useful for evaluating autonomic innervation and dysregulation in PAD and MVD [176–178]. Although the short half-life of [^{11}C]HED and the requirement for an on-site cyclotron present significant limitations for widespread clinical application in PAD, the use of a longer half-life sympathetic targeted radiotracer like [^{18}F]LMI1195 could overcomes these limitations [176–178]. The role of sympathetic innervation in modulating microcirculatory physiology and PAD pathogenesis remains to be fully explored.

5. Conclusion

Physiological and molecular imaging of the microcirculation holds promise in the detection, classification, and management of PAD and for enhancing our understanding of the pathophysiology of PAD. Current imaging modalities offer a wide array of approaches to elucidate the role of MVD in preclinical and clinical studies of PAD. Assessment of MVD could yield the development of refined risk stratification models, providing improved selection of those most likely to respond to revascularization, and assessment of efficacy of interventions, and prediction of amputation and mortality. The implementation of imaging modalities to further expand our understanding of microcirculation in PAD will significantly change the field in the upcoming decades and bring the evaluation of MVD to the forefront of the assessment of PAD.

Disclosures

Dr. Mena-Hurtado reports unrestricted research grants from Philips and Shockwave and is a consultant for Abbott Vascular, Cook, Optum Labs; Dr. Smolderen reports unrestricted research grants from Philips,

Merck, Shockwave, and Johnson & Johnson; she is a consultant for Optum Labs, Cook, Tegus, Twill Inc. and Abbott Vascular. Albert J. Sinusas reports Institutional grants from Jubilant and Siemens; individual consulting fees unrelated to PET imaging compounds from MicroVide, LLC; patents related to SPECT imaging agent RP805 for MicroVide, LLC; member Cardiovascular Council of SNMMI (no funds received); receipt of equipment, materials, drugs, or other services from Lantheus (MTA LMI1195) and Jubilant (Rb-82 generator). The other authors declare no relevant conflict of interest.

Sources of funding

Albert J. Sinusas reports NIH funding related to this article (R01HL163640).

CRediT authorship contribution statement

Santiago Callegari: Conceptualization, Investigation, Writing – original draft, Writing – review & editing. **Attila Feher:** Conceptualization, Investigation, Writing – original draft, Writing – review & editing. **Kim G. Smolderen:** Conceptualization, Funding acquisition, Writing – review & editing, Supervision. **Carlos Mena-Hurtado:** Conceptualization, Visualization, Writing – review & editing, Supervision. **Albert J. Sinusas:** Conceptualization, Investigation, Methodology, Supervision, Visualization, Writing – review & editing, Funding acquisition.

Declaration of competing interest

The authors declare the following financial interests/personal relationships which may be considered as potential competing interests: Albert J. Sinusas reports financial support was provided by National Institutes of Health. Carlos Mena-Hurtado reports a relationship with Phillips that includes: funding grants. Carlos Mena-Hurtado reports a relationship with Shockwave Medical Inc. that includes: funding grants. Carlos Mena-Hurtado reports a relationship with Abbott Vascular Inc. that includes: consulting or advisory. Carlos Mena-Hurtado reports a relationship with Cook Medical Inc. that includes: consulting or advisory. Carlos Mena-Hurtado reports a relationship with Optum Labs Inc. that includes: consulting or advisory. Kim G. Smolderen reports a relationship with Phillips that includes: funding grants. Kim G. Smolderen reports a relationship with Merck that includes: funding grants. Kim G. Smolderen reports a relationship with Shockwave Medical Inc. that includes: funding grants. Kim G. Smolderen reports a relationship with Johnson & Johnson Inc. that includes: funding grants. Kim G. Smolderen reports a relationship with Optum Labs Inc. that includes: consulting or advisory. Kim G. Smolderen reports a relationship with Cook Medical Inc. that includes: consulting or advisory. Kim G. Smolderen reports a relationship with Tegus that includes: consulting or advisory. Kim G. Smolderen reports a relationship with Twill Inc. that includes: consulting or advisory. Kim G. Smolderen reports a relationship with Abbott Vascular Inc. that includes: consulting or advisory. Albert J. Sinusas reports a relationship with Jubilant Inc. that includes: consulting or advisory. Albert J. Sinusas reports a relationship with SIEMENS that includes: consulting or advisory. Albert J. Sinusas reports a relationship with MicroVide, LLC that includes: consulting or advisory. Albert J. Sinusas is a member Cardiovascular Council of SNMMI (no funds received); receipt of equipment, materials, drugs, or other services from Lantheus (MTA LMI1195) and Jubilant (Rb-82 generator). If there are other authors, they declare that they have no known competing financial interests or personal relationships that could have appeared to influence the work reported in this paper.

References

[1] P. Song, Z. Fang, H. Wang, Y. Cai, K. Rahimi, Y. Zhu, et al., Global and regional prevalence, burden, and risk factors for carotid atherosclerosis: a systematic review, meta-analysis, and modelling study, Lancet Glob. Health 8 (5) (2020) e721–e729.
[2] C.W. Tsao, A.W. Aday, Z.I. Almarzooq, C.A.M. Anderson, P. Arora, C.L. Avery, et al., Heart disease and stroke statistics-2023 update: a report from the American Heart Association, Circulation 147 (8) (2023) e93–e621.
[3] M.H. Criqui, K. Matsushita, V. Aboyans, C.N. Hess, C.W. Hicks, T.W. Kwan, et al., Lower extremity peripheral artery disease: contemporary epidemiology, management gaps, and future directions: a scientific statement from the American Heart Association, Circulation 144 (9) (2021) e171–e191.
[4] T.S. Polonsky, M.M. McDermott, Lower extremity peripheral artery disease without chronic limb-threatening ischemia: a review, JAMA 325 (21) (2021) 2188–2198.
[5] A.W. Aday, K. Matsushita, Epidemiology of peripheral artery disease and polyvascular disease, Circ. Res. 128 (12) (2021) 1818–1832.
[6] S. Subherwal, M.R. Patel, L. Kober, E.D. Peterson, D.L. Bhatt, G.H. Gislason, et al., Peripheral artery disease is a coronary heart disease risk equivalent among both men and women: results from a nationwide study, Eur. J. Prev. Cardiol. 22 (3) (2015) 317–325.
[7] J.A. Beckman, M.S. Duncan, S.M. Damrauer, Q.S. Wells, J.V. Barnett, D. H. Wasserman, et al., Microvascular disease, peripheral artery disease, and amputation, Circulation 140 (6) (2019) 449–458.
[8] M.A. Creager, K. Matsushita, S. Arya, J.A. Beckman, S. Duval, P.P. Goodney, et al., Reducing nontraumatic lower-extremity amputations by 20% by 2030: time to get to our feet: a policy statement from the American Heart Association, Circulation 143 (17) (2021) e875–e891.
[9] D.J. Adam, J.D. Beard, T. Cleveland, J. Bell, A.W. Bradbury, J.F. Forbes, et al., Bypass versus angioplasty in severe ischaemia of the leg (BASIL): multicentre, randomised controlled trial, Lancet 366 (9501) (2005) 1925–1934.
[10] K.G. Smolderen, O. Alabi, T.C. Collins, B. Dennis, P.P. Goodney, C. Mena-Hurtado, et al., Advancing peripheral artery disease quality of care and outcomes through patient-reported health status assessment: a scientific statement from the American Heart Association, Circulation 146 (20) (2022) e286–e297.
[11] J.R. Stern, C.K. Wong, M. Yerovinkina, S.J. Spindler, A.S. See, S. Panjaki, et al., A meta-analysis of long-term mortality and associated risk factors following lower extremity amputation, Ann. Vasc. Surg. 42 (2017) 322–327.
[12] A. Wu, J. Coresh, E. Selvin, H. Tanaka, G. Heiss, A.T. Hirsch, et al., Lower extremity peripheral artery disease and quality of life among older individuals in the community, J. Am. Heart Assoc. 6 (1) (2017).
[13] A.T. Tran, J.A. Spertus, C.I. Mena-Hurtado, P.G. Jones, H.D. Aronow, D.M. Safley, et al., Association of disease-specific health status with long-term survival in peripheral artery disease, J. Am. Heart Assoc. 11 (4) (2022) e022232.
[14] K.G. Smolderen, Z. Samaan, B. Ward-Zimmerman, L. Fucito, P. Goodney, V. Le, et al., Integrating psychosocial care in the management of patients with vascular disease, J. Am. Coll. Cardiol. 81 (12) (2023) 1201–1204.
[15] K.M. Harris, C. Mena-Hurtado, M.M. Burg, P.W. Vriens, J. Heyligers, K. G. Smolderen, Association of depression and anxiety disorders with outcomes after revascularization in chronic limb-threatening ischemia hospitalizations nationwide, J. Vasc. Surg. 77 (2) (2023) 480–489.
[16] A. Behroozian, J.A. Beckman, Microvascular disease increases amputation in patients with peripheral artery disease, Arterioscler. Thromb. Vasc. Biol. 40 (3) (2020) 534–540.
[17] Johnson BL, Glickman MH, Bandyk DF, Esses GE. Failure of foot salvage in patients with end-stage renal disease after surgical revascularization. J. Vasc. Surg. 1995;22(3):280–5; discussion 285–6.
[18] A. Caselli, V. Latini, A. Lapenna, S. Di Carlo, F. Pirozzi, A. Benvenuto, et al., Transcutaneous oxygen tension monitoring after successful revascularization in diabetic patients with ischaemic foot ulcers, Diabet. Med. 22 (4) (2005) 460–465.
[19] K.G. Smolderen, G. Romain, J.B. Provance, L.E. Scierka, J. Mao, P.P. Goodney, et al., Guideline-directed medical therapy and long-term mortality and amputation outcomes in patients undergoing peripheral vascular interventions, JACC Cardiovasc. Interv. 16 (3) (2023) 332–343.
[20] J.A. Beckman, P.A. Schneider, M.S. Conte, Advances in revascularization for peripheral artery disease: revascularization in PAD, Circ. Res. 128 (12) (2021) 1885–1912.
[21] M.A. Hussain, M. Al-Omran, K. Salata, A. Sivaswamy, T.L. Forbes, N. Sattar, et al., Population-based secular trends in lower-extremity amputation for diabetes and peripheral artery disease, CMAJ 191 (35) (2019) E955–E961.
[22] R. Stein, I. Hriljac, J.L. Halperin, S.M. Gustavson, V. Teodorescu, J.W. Olin, Limitation of the resting ankle-brachial index in symptomatic patients with peripheral arterial disease, Vasc. Med. 11 (1) (2006) 29–33.
[23] A.F. AbuRahma, E. Adams, J. AbuRahma, L.A. Mata, L.S. Dean, C. Caron, et al., Critical analysis and limitations of resting ankle-brachial index in the diagnosis of symptomatic peripheral arterial disease patients and the role of diabetes mellitus and chronic kidney disease, J. Vasc. Surg. 71 (3) (2020) 937–945.
[24] D. Blanca, E.C. Schwarz, T.J. Olgers, E. Ter Avest, N. Azizi, H.R. Bouma, et al., Intra-and inter-observer variability of point of care ultrasound measurements to evaluate hemodynamic parameters in healthy volunteers, Ultrasound J. 15 (1) (2023) 22.
[25] A. Alashi, B.C. Vermillion, A.J. Sinusas, The potential role of PET in the management of peripheral artery disease, Curr. Cardiol. Rep. 25 (8) (2023) 831–839.

[26] F. Zurlo, K. Larson, C. Bogardus, E. Ravussin, Skeletal muscle metabolism is a major determinant of resting energy expenditure, J. Clin. Invest. 86 (5) (1990) 1423–1427.
[27] A. Feher, A.J. Sinusas, Quantitative assessment of coronary microvascular function: dynamic single-photon emission computed tomography, positron emission tomography, ultrasound, computed tomography, and magnetic resonance imaging, Circ. Cardiovasc. Imaging 10 (8) (2017).
[28] G.C. Gaitanos, C. Williams, L.H. Boobis, S. Brooks, Human muscle metabolism during intermittent maximal exercise, J. Appl. Physiol. (1985) 75 (2) (1993) 712–719.
[29] P. Andersen, B. Saltin, Maximal perfusion of skeletal muscle in man, J. Physiol. 366 (1985) 233–249.
[30] M.J. Gibala, M.A. Tarnopolsky, T.E. Graham, Tricarboxylic acid cycle intermediates in human muscle at rest and during prolonged cycling, Am. J. Physiol. 272 (2 Pt 1) (1997) E239–E244.
[31] B. Egan, J.R. Zierath, Exercise metabolism and the molecular regulation of skeletal muscle adaptation, Cell Metab. 17 (2) (2013) 162–184.
[32] D. Thiebaud, E. Jacot, R.A. DeFronzo, E. Maeder, E. Jequier, J.P. Felber, The effect of graded doses of insulin on total glucose uptake, glucose oxidation, and glucose storage in man, Diabetes 31 (11) (1982) 957–963.
[33] R.A. DeFronzo, D. Tripathy, Skeletal muscle insulin resistance is the primary defect in type 2 diabetes, Diabetes Care 32 Suppl 2(Suppl 2) (2009) S157–S163.
[34] S.B. Rutkove, S. Callegari, H. Concepcion, T. Mourey, J. Widrick, J.A. Nagy, et al., Electrical impedance myography detects age-related skeletal muscle atrophy in adult zebrafish, Sci. Rep. 13 (1) (2023) 7191.
[35] M.M. McDermott, L. Ferrucci, M. Gonzalez-Freire, K. Kosmac, C. Leeuwenburgh, C.A. Peterson, et al., Skeletal muscle pathology in peripheral artery disease: a brief review, Arterioscler. Thromb. Vasc. Biol. 40 (11) (2020) 2577–2585.
[36] P. Mishra, G. Varuzhanyan, A.H. Pham, D.C. Chan, Mitochondrial dynamics is a distinguishing feature of skeletal muscle fiber types and regulates organellar compartmentalization, Cell Metab. 22 (6) (2015) 1033–1044.
[37] P. Koutakis, D.J. Weiss, D. Miserlis, V.K. Shostrom, E. Papoutsi, D.M. Ha, et al., Oxidative damage in the gastrocnemius of patients with peripheral artery disease is myofiber type selective, Redox Biol. 2 (2014) 921–928.
[38] J.G. Regensteiner, E.E. Wolfel, E.P. Brass, M.R. Carry, S.P. Ringel, M.E. Hargarten, et al., Chronic changes in skeletal muscle histology and function in peripheral arterial disease, Circulation 87 (2) (1993) 413–421.
[39] B. Glancy, L.Y. Hsu, L. Dao, M. Bakalar, S. French, D.J. Chess, et al., In vivo microscopy reveals extensive embedding of capillaries within the sarcolemma of skeletal muscle fibers, Microcirculation 21 (2) (2014) 131–147.
[40] S.H. White, M.M. McDermott, R.L. Sufit, K. Kosmac, A.W. Bugg, M. Gonzalez-Freire, et al., Walking performance is positively correlated to calf muscle fiber size in peripheral artery disease subjects, but fibers show aberrant mitophagy: an observational study, J. Transl. Med. 14 (1) (2016) 284.
[41] C. Hillier, R.D. Sayers, P.A. Watt, R. Naylor, P.R. Bell, H. Thurston, Altered small artery morphology and reactivity in critical limb ischaemia, Clin. Sci. (Lond.) 96 (2) (1999) 155–163.
[42] F.W. Sellke, M.L. Armstrong, D.G. Harrison, Endothelium-dependent vascular relaxation is abnormal in the coronary microcirculation of atherosclerotic primates, Circulation 81 (5) (1990) 1586–1593.
[43] H. Yin, J.M. Arpino, J.J. Lee, J.G. Pickering, Regenerated microvascular networks in ischemic skeletal muscle, Front. Physiol. 12 (2021) 662073.
[44] N.T. Kruse, K. Ueda, W.E. Hughes, D.P. Casey, Eight weeks of nitrate supplementation improves blood flow and reduces the exaggerated pressor response during forearm exercise in peripheral artery disease, Am. J. Physiol. Heart Circ. Physiol. 315 (1) (2018) H101–H108.
[45] O. Baum, M. Bigler, Pericapillary basement membrane thickening in human skeletal muscles, Am. J. Physiol. Heart Circ. Physiol. 311 (3) (2016) H654–H666.
[46] T.K. Ho, V. Rajkumar, C.M. Black, D.J. Abraham, D.M. Baker, Increased angiogenic response but deficient arteriolization and abnormal microvessel ultrastructure in critical leg ischaemia, Br. J. Surg. 93 (11) (2006) 1368–1376.
[47] O. Baum, V. Djonov, M. Ganster, M. Widmer, I. Baumgartner, Arteriolization of capillaries and FGF-2 upregulation in skeletal muscles of patients with chronic peripheral arterial disease, Microcirculation 12 (6) (2005) 527–537.
[48] C.D. Askew, S. Green, P.J. Walker, G.K. Kerr, A.A. Green, A.D. Williams, et al., Skeletal muscle phenotype is associated with exercise tolerance in patients with peripheral arterial disease, J. Vasc. Surg. 41 (5) (2005) 802–807.
[49] O. Baum, E. Torchetti, C. Malik, B. Hoier, M. Walker, P.J. Walker, et al., Capillary ultrastructure and mitochondrial volume density in skeletal muscle in relation to reduced exercise capacity of patients with intermittent claudication, Am. J. Physiol. Regul. Integr. Comp. Physiol. 310 (10) (2016) R943–R951.
[50] W.S. Jones, B.D. Duscha, J.L. Robbins, N.N. Duggan, J.G. Regensteiner, W. E. Kraus, et al., Alteration in angiogenic and anti-angiogenic forms of vascular endothelial growth factor-a in skeletal muscle of patients with intermittent claudication following exercise training, Vasc. Med. 17 (2) (2012) 94–100.
[51] J.L. Robbins, W.S. Jones, B.D. Duscha, J.D. Allen, W.E. Kraus, J.G. Regensteiner, et al., Relationship between leg muscle capillary density and peak hyperemic blood flow with endurance capacity in peripheral artery disease, J. Appl. Physiol. (1985) 111 (1) (2011) 81–86.
[52] B.D. Duscha, W.E. Kraus, W.S. Jones, J.L. Robbins, L.W. Piner, K.M. Huffman, et al., Skeletal muscle capillary density is related to anaerobic threshold and claudication in peripheral artery disease, Vasc. Med. 25 (5) (2020) 411–418.
[53] M. Bethel, Brian H. Annex, Peripheral arterial disease: a small and large vessel problem. American Heart Journal Plus, Cardiol. Res. Pract. (2023) 28.
[54] A.J. Flammer, T. Anderson, D.S. Celermajer, M.A. Creager, J. Deanfield, P. Ganz, et al., The assessment of endothelial function: from research into clinical practice, Circulation 126 (6) (2012) 753–767.
[55] A.L. Huang, A.E. Silver, E. Shvenke, D.W. Schopfer, E. Jahangir, M.A. Titas, et al., Predictive value of reactive hyperemia for cardiovascular events in patients with peripheral arterial disease undergoing vascular surgery, Arterioscler. Thromb. Vasc. Biol. 27 (10) (2007) 2113–2119.
[56] R. Rosenberry, M.D. Nelson, Reactive hyperemia: a review of methods, mechanisms, and considerations, Am. J. Physiol. Regul. Integr. Comp. Physiol. 318 (3) (2020) R605–R618.
[57] D.D. Gutterman, D.S. Chabowski, A.O. Kadlec, M.J. Durand, J.K. Freed, K. Ait-Aissa, et al., The human microcirculation: regulation of flow and beyond, Circ. Res. 118 (1) (2016) 157–172.
[58] J.M. Greve, S.P. Williams, L.J. Bernstein, H. Goldman, F.V. Peale Jr., S. Bunting, et al., Reactive hyperemia and BOLD MRI demonstrate that VEGF inhibition, age, and atherosclerosis adversely affect functional recovery in a murine model of peripheral artery disease, J. Magn. Reson. Imaging 28 (4) (2008) 996–1004.
[59] V. Bartoli, B. Dorigo, Comparison between reactive and exercise hyperemia in normal subjects and patients with peripheral arterial disease, Angiology 30 (1) (1979) 40–47.
[60] S. Kiani, J.G. Aasen, M. Holbrook, A. Khemka, F. Sharmeen, R.M. LeLeiko, et al., Peripheral artery disease is associated with severe impairment of vascular function, Vasc. Med. 18 (2) (2013) 72–78.
[61] E. Amarteifio, M.A. Weber, S. Wormsbecher, S. Demirel, H. Krakowski-Roosen, A. Jores, et al., Dynamic contrast-enhanced ultrasound for assessment of skeletal muscle microcirculation in peripheral arterial disease, Invest. Radiol. 46 (8) (2011) 504–508.
[62] D. Duerschmied, L. Olson, M. Olschewski, A. Rossknecht, G. Freund, C. Bode, et al., Contrast ultrasound perfusion imaging of lower extremities in peripheral arterial disease: a novel diagnostic method, Eur. Heart J. 27 (3) (2006) 310–315.
[63] A.L. Meneses, M.C.Y. Nam, T.G. Bailey, R. Magee, J. Golledge, Y. Hellsten, et al., Leg blood flow and skeletal muscle microvascular perfusion responses to submaximal exercise in peripheral arterial disease, Am. J. Physiol. Heart Circ. Physiol. 315 (5) (2018) H1425–H1433.
[64] E. Murphy, J. Rocha, N. Gildea, S. Green, M. Egana, Venous occlusion plethysmography vs. Doppler ultrasound in the assessment of leg blood flow kinetics during different intensities of calf exercise, Eur. J. Appl. Physiol. 118 (2) (2018) 249–260.
[65] A. Meneses, D. Krastins, M. Nam, T. Bailey, J. Quah, V. Sankhla, et al., Toward a better understanding of muscle microvascular perfusion during exercise in patients with peripheral artery disease: the effect of lower-limb revascularization, J. Endovasc. Ther. 31 (2022) 115–125, 15266028221114722.
[66] O.R. Mason, B.P. Davidson, P. Sheeran, M. Muller, J.M. Hodovan, J. Sutton, et al., Augmentation of tissue perfusion in patients with peripheral artery disease using microbubble cavitation, JACC Cardiovasc. Imaging 13 (3) (2020) 641–651.
[67] C. Jagren, B. Gazelius, C. Ihrman-Sandal, L.E. Lindblad, J. Ostergren, Skin microvascular dilatation response to acetylcholine and sodium nitroprusside in peripheral arterial disease, Clin. Physiol. Funct. Imaging 22 (6) (2002) 370–374.
[68] M. Akkoca, S.E. Usanmaz, C. Koksoy, U. Bengisun, E. Demirel-Yilmaz, Plasma nitric oxide level is correlated with microvascular functions in the peripheral arterial disease, Clin. Hemorheol. Microcirc. 65 (2) (2017) 151–162.
[69] M.A. Fuglestad, H. Hernandez, Y. Gao, H. Ybay, M.N. Schieber, K.E. Brunette, et al., A low-cost, wireless near-infrared spectroscopy device detects the presence of lower extremity atherosclerosis as measured by computed tomographic angiography and characterizes walking impairment in peripheral artery disease, J. Vasc. Surg. 71 (3) (2020) 946–957.
[70] S. Joseph, B. Munshi, R. Agarini, R.C.H. Kwok, D.J. Green, S. Jansen, Near infrared spectroscopy in peripheral artery disease and the diabetic foot: a systematic review, Diabetes Metab. Res. Rev. 38 (7) (2022) e3571.
[71] T. Baltrunas, V. Mosenko, A. Mackevicius, V. Dambrauskas, I. Asakiene, K. Rucinskas, et al., The use of near-infrared spectroscopy in the diagnosis of peripheral artery disease: a systematic review, Vascular 30 (4) (2022) 715–727.
[72] J.R. Murrow, J.T. Brizendine, B. Djire, H.J. Young, S. Rathbun, K.R. Nilsson Jr., et al., Near infrared spectroscopy-guided exercise training for claudication in peripheral arterial disease, Eur. J. Prev. Cardiol. 26 (5) (2019) 471–480.
[73] N. Cornelis, P. Chatzinikolaou, R. Buys, I. Fourneau, J. Claes, V. Cornelissen, The use of near infrared spectroscopy to evaluate the effect of exercise on peripheral muscle oxygenation in patients with lower extremity artery disease: a systematic review, Eur. J. Vasc. Endovasc. Surg. 61 (5) (2021) 837–847.
[74] C. Weinkauf, A. Mazhar, K. Vaishnav, A.A. Hamadani, D.J. Cuccia, D. G. Armstrong, Near-instant noninvasive optical imaging of tissue perfusion for vascular assessment, J. Vasc. Surg. 69 (2) (2019) 555–562.
[75] K.J. Zuzak, M.D. Schaeberle, E.N. Lewis, I.W. Levin, Visible reflectance hyperspectral imaging: characterization of a noninvasive, in vivo system for determining tissue perfusion, Anal. Chem. 74 (9) (2002) 2021–2028.
[76] M.A. Calin, T. Coman, S.V. Parasca, N. Bercaru, R. Savastru, D. Manea, Hyperspectral imaging-based wound analysis using mixture-tuned matched filtering classification method, J. Biomed. Opt. 20 (4) (2015) 046004.
[77] H. Fabelo, S. Ortega, D. Ravi, B.R. Kiran, C. Sosa, D. Bulters, et al., Spatio-spectral classification of hyperspectral images for brain cancer detection during surgical operations, PloS One 13 (3) (2018) e0193721.
[78] B. Jansen-Winkeln, M. Maktabi, J.P. Takoh, S.M. Rabe, M. Barberio, H. Kohler, et al., Hyperspectral imaging of gastrointestinal anastomoses, Chirurg 89 (9) (2018) 717–725.

[79] E. Grambow, M. Dau, A. Holmer, V. Lipp, B. Frerich, E. Klar, et al., Hyperspectral imaging for monitoring of perfusion failure upon microvascular anastomosis in the rat hind limb, Microvasc. Res. 116 (2018) 64–70.
[80] E. Grambow, M. Dau, N.A. Sandkuhler, M. Leuchter, A. Holmer, E. Klar, et al., Evaluation of peripheral artery disease with the TIVITA(R) tissue hyperspectral imaging camera system, Clin. Hemorheol. Microcirc. 73 (1) (2019) 3–17.
[81] M.R. Stacy, C.M. Caracciolo, M. Qiu, P. Pal, T. Varga, R.T. Constable, et al., Comparison of regional skeletal muscle tissue oxygenation in college athletes and sedentary control subjects using quantitative BOLD MR imaging, Physiol. Rep. 4 (16) (2016).
[82] S. Suo, H. Tang, Q. Lu, L. Zhang, Q. Ni, M. Cao, et al., Blood oxygenation level-dependent cardiovascular magnetic resonance of the skeletal muscle in healthy adults: different paradigms for provoking signal alterations, Magn. Reson. Med. 85 (3) (2021) 1590–1601.
[83] M.R. Stacy, Molecular imaging of lower extremity peripheral arterial disease: an emerging field in nuclear medicine, Front. Med. (Lausanne) 8 (2021) 793975.
[84] M.R. Stacy, M. Qiu, X. Papademetris, C.M. Caracciolo, R.T. Constable, A. J. Sinusas, Application of BOLD magnetic resonance imaging for evaluating regional volumetric foot tissue oxygenation: a feasibility study in healthy volunteers, Eur. J. Vasc. Endovasc. Surg. 51 (5) (2016) 743–749.
[85] M. Guerraty, A. Bhargava, J. Senarathna, A.A. Mendelson, A.P. Pathak, Advances in translational imaging of the microcirculation, Microcirculation 28 (3) (2021) e12683.
[86] H.P. Ledermann, A.C. Schulte, H.G. Heidecker, M. Aschwanden, K.A. Jager, K. Scheffler, et al., Blood oxygenation level-dependent magnetic resonance imaging of the skeletal muscle in patients with peripheral arterial occlusive disease, Circulation 113 (25) (2006) 2929–2935.
[87] B. Jacobi, G. Bongartz, S. Partovi, A.C. Schulte, M. Aschwanden, A.B. Lumsden, et al., Skeletal muscle BOLD MRI: from underlying physiological concepts to its usefulness in clinical conditions, J. Magn. Reson. Imaging 35 (6) (2012) 1253–1265.
[88] D.S. Williams, J.A. Detre, J.S. Leigh, A.P. Koretsky, Magnetic resonance imaging of perfusion using spin inversion of arterial water, Proc. Natl. Acad. Sci. U. S. A. 89 (1) (1992) 212–216.
[89] W.C. Wu, E. Mohler 3rd, S.J. Ratcliffe, F.W. Wehrli, J.A. Detre, T.F. Floyd, Skeletal muscle microvascular flow in progressive peripheral artery disease: assessment with continuous arterial spin-labeling perfusion magnetic resonance imaging, J. Am. Coll. Cardiol. 53 (25) (2009) 2372–2377.
[90] A.W. Pollak, C.H. Meyer, F.H. Epstein, R.S. Jiji, J.R. Hunter, J.M. Dimaria, et al., Arterial spin labeling MR imaging reproducibly measures peak-exercise calf muscle perfusion: a study in patients with peripheral arterial disease and healthy volunteers, JACC Cardiovasc. Imaging 5 (12) (2012) 1224–1230.
[91] R.C. Mathew, C.M. Kramer, Recent advances in magnetic resonance imaging for peripheral artery disease, Vasc. Med. 23 (2) (2018) 143–152.
[92] D. Le Bihan, What can we see with IVIM MRI? Neuroimage 187 (2019) 56–67.
[93] M. Iima, D. Le Bihan, Clinical intravoxel incoherent motion and diffusion MR imaging: past, present, and future, Radiology 278 (1) (2016) 13–32.
[94] N. Galanakis, T.G. Maris, G. Kalaitzakis, N. Kontopodis, N. Matthaiou, S. Charalambous, et al., Evaluation of foot hypoperfusion and estimation of percutaneous transluminal angioplasty outcome in patients with critical limb ischemia using intravoxel incoherent motion microperfusion MRI, Br. J. Radiol. 94 (1125) (2021) 20210215.
[95] H. Tang, L. Yu, S. Suo, Y. Hu, J. Wang, J. Xu, et al., Evaluation of skeletal muscle perfusion changes in patients with peripheral artery disease before and after percutaneous transluminal angioplasty using multiparametric MR imaging, Magn. Reson. Imaging 93 (2022) 157–162.
[96] J. Butler, G.M. Rocker, S. Westaby, Inflammatory response to cardiopulmonary bypass, Ann. Thorac. Surg. 55 (2) (1993) 552–559.
[97] O.A. Gimnich, T. Belousova, C.M. Short, A.A. Taylor, V. Nambi, J.D. Morrisett, et al., Magnetic resonance imaging-derived microvascular perfusion modeling to assess peripheral artery disease, J. Am. Heart Assoc. 12 (3) (2023) e027649.
[98] S. Suo, L. Zhang, H. Tang, Q. Ni, S. Li, H. Mao, et al., Evaluation of skeletal muscle microvascular perfusion of lower extremities by cardiovascular magnetic resonance arterial spin labeling, blood oxygenation level-dependent, and intravoxel incoherent motion techniques, J. Cardiovasc. Magn. Reson. 20 (1) (2018) 18.
[99] Y.C. Lin, T.C. Fu, G. Lin, S.H. Ng, C.H. Yeh, S.C. Ng, et al., Using T1 mapping indices to evaluate muscle function and predict conservative treatment outcomes in diabetic patients with peripheral arterial disease, Eur. Radiol. 33 (7) (2023) 4927–4937.
[100] Y.C. Lin, W.Y. Chuang, F.C. Wei, C.H. Yeh, I. Tinhofer, N.F. Al Deek, et al., Peripheral arterial disease: the role of extracellular volume measurements in lower limb muscles with MRI, Eur. Radiol. 30 (7) (2020) 3943–3950.
[101] P. Haaf, P. Garg, D.R. Messroghli, D.A. Broadbent, J.P. Greenwood, S. Plein, Cardiac T1 mapping and extracellular volume (ECV) in clinical practice: a comprehensive review, J. Cardiovasc. Magn. Reson. 18 (1) (2016) 89.
[102] R.T. George, M. Jerosch-Herold, C. Silva, K. Kitagawa, D.A. Bluemke, J.A. Lima, et al., Quantification of myocardial perfusion using dynamic 64-detector computed tomography, Invest. Radiol. 42 (12) (2007) 815–822.
[103] F. Bamberg, R. Hinkel, R.P. Marcus, E. Baloch, K. Hildebrandt, F. Schwarz, et al., Feasibility of dynamic CT-based adenosine stress myocardial perfusion imaging to detect and differentiate ischemic and infarcted myocardium in an large experimental porcine animal model, Int. J. Cardiovasc. Imaging 30 (4) (2014) 803–812.
[104] E. Tonet, G. Pompei, E. Faragasso, A. Cossu, R. Pavasini, G. Passarini, et al., Coronary microvascular dysfunction: PET, CMR and CT assessment, J. Clin. Med. 10 (9) (2021).
[105] M.B. Moller, P. Hasbak, J.J. Linde, P.E. Sigvardsen, L.V. Kober, K.F. Kofoed, Quantification of myocardial blood flow using dynamic myocardial CT perfusion compared with (82)Rb PET, J. Cardiovasc. Comput. Tomogr. 17 (3) (2023) 185–191.
[106] A.M. Alessio, M. Bindschadler, J.M. Busey, W.P. Shuman, J.H. Caldwell, K. R. Branch, Accuracy of myocardial blood flow estimation from dynamic contrast-enhanced cardiac CT compared with PET, Circ. Cardiovasc. Imaging 12 (6) (2019) e008323.
[107] P. Veit-Haibach, M.W. Huellner, M. Banyai, S. Mafeld, J. Heverhagen, K. Strobel, et al., CT perfusion in peripheral arterial disease-hemodynamic differences before and after revascularisation, Eur. Radiol. 31 (8) (2021) 5507–5513.
[108] N. Galanakis, T.G. Maris, N. Kontopodis, C.V. Ioannou, E. Kehagias, N. Matthaiou, et al., CT foot perfusion examination for evaluation of percutaneous transluminal angioplasty outcome in patients with critical limb ischemia: a feasibility study, J. Vasc. Interv. Radiol. 30 (4) (2019) 560–568.
[109] M. Li, Z. Li, P. Gao, L. Jin, L. Li, W. Zhao, et al., Quantitative evaluation of postintervention foot blood supply in patients with peripheral artery disease by computed tomography perfusion, J. Vasc. Surg. 72 (3) (2020) 1035–1042.
[110] A. Feher, N.E. Boutagy, J.C. Stendahl, C. Hawley, N. Guerrera, C.J. Booth, et al., Computed tomographic angiography assessment of epicardial coronary vasoreactivity for early detection of doxorubicin-induced cardiotoxicity, JACC CardioOncol 2 (2) (2020) 207–219.
[111] D. De Santis, C.N. De Cecco, U.J. Schoepf, J.W. Nance, R.T. Yamada, B.A. Thomas, et al., Modified calcium subtraction in dual-energy CT angiography of the lower extremity runoff: impact on diagnostic accuracy for stenosis detection, Eur. Radiol. 29 (9) (2019) 4783–4793.
[112] B.C. Meyer, T. Werncke, W. Hopfenmuller, H.J. Raatschen, K.J. Wolf, T. Albrecht, Dual energy CT of peripheral arteries: effect of automatic bone and plaque removal on image quality and grading of stenoses, Eur. J. Radiol. 68 (3) (2008) 414–422.
[113] N.M. Meyersohn, T.G. Walker, G.R. Oliveira, Advances in axial imaging of peripheral vascular disease, Curr. Cardiol. Rep. 17 (10) (2015) 87.
[114] H.B.U.I. Sayman, Muscle perfusion with technetium-MIBI in lower extremity peripheral arte- rial diseases, J. Nucl. Med. 32 (9) (1991) 1700–1703.
[115] J.S. Seder, E.H. Botvinick, S.H. Rahimtoola, J. Goldstone, D.C. Price, Detecting and localizing peripheral arterial disease: assessment of 201Tl scintigraphy, AJR Am. J. Roentgenol. 137 (2) (1981) 373–380.
[116] M.Y.M. Miyamoto, H. Takano, et al., Therapeu- tic angiogenesis by autologous bone marrow cell implantation for refractory chronic peripheral arterial disease using assessment of neovascularization by 99mTc-tetrofosmin (TF) perfusion scintigraphy, Cell Transplant. 13 (4) (2004) 429–437.
[117] M.R. Stacy, W. Zhou, A.J. Sinusas, Radiotracer imaging of peripheral vascular disease, J. Nucl. Med. 54 (12) (2013) 2104–2110.
[118] M.R. Stacy, A.J. Sinusas, Novel applications of radionuclide imaging in peripheral vascular disease, Cardiol. Clin. 34 (1) (2016) 167–177.
[119] J.L. Alvelo, X. Papademetris, C. Mena-Hurtado, S. Jeon, B.E. Sumpio, A.J. Sinusas, et al., Radiotracer imaging allows for noninvasive detection and quantification of abnormalities in angiosome foot perfusion in diabetic patients with critical limb ischemia and nonhealing wounds, Circ. Cardiovasc. Imaging 11 (5) (2018) e006932.
[120] T.H. Chou, J.L. Alvelo, S. Janse, X. Papademetris, B.E. Sumpio, C. Mena-Hurtado, et al., Prognostic value of radiotracer-based perfusion imaging in critical limb ischemia patients undergoing lower extremity revascularization, JACC Cardiovasc. Imaging 14 (8) (2021) 1614–1624.
[121] W.S.S. Burchert, J. van den Hoff, Oxygen-15-water PET assessment of muscular blood flow in peripheral vascular disease, J. Nucl. Med. 37 (1996) 93–98.
[122] A.J.H.H. Fischman, E.A. Carter, et al., Regional mea- surement of canine skeletal muscle blood flow by positron emission tomography with H2(15)O. J Appl Physiol (1985) 2002;92(4):1709–16. Regional mea- surement of canine skeletal muscle blood flow by positron emission tomography with H2(15)O, J. Appl. Physiol. 92 (4) (2002) 1709–1716.
[123] Penuelas I. AX, G. Abizanda, (13)N- ammonia PET as a measurement of hindlimb perfusion in a mouse model of peripheral artery occlusive disease, J. Nucl. Med. 48 (7) (2007) 1216–1223.
[124] I. Penuelas, X.L. Aranguren, G. Abizanda, J.M. Marti-Climent, M. Uriz, M. Ecay, et al., (13)N-ammonia PET as a measurement of hindlimb perfusion in a mouse model of peripheral artery occlusive disease, J. Nucl. Med. 48 (7) (2007) 1216–1223.
[125] K.K. Kalliokoski, J. Knuuti, P. Nuutila, Relationship between muscle blood flow and oxygen uptake during exercise in endurance-trained and untrained men, J. Appl. Physiol. (1985) 98 (1) (2005) 380–383.
[126] O.U. Scremin, S.F. Figoni, K. Norman, A.M. Scremin, C.F. Kunkel, D. Opava-Rutter, et al., Preamputation evaluation of lower-limb skeletal muscle perfusion with H(2) (15)O positron emission tomography, Am. J. Phys. Med. Rehabil. 89 (6) (2010) 473–486.
[127] J.O. Prior, G. Allenbach, I. Valenta, M. Kosinski, C. Burger, F.R. Verdun, et al., Quantification of myocardial blood flow with 82Rb positron emission tomography: clinical validation with 15O-water, Eur. J. Nucl. Med. Mol. Imaging 39 (6) (2012) 1037–1047.
[128] J. Maddahi, D. Agostini, T.M. Bateman, J.J. Bax, R.S.B. Beanlands, D.S. Berman, et al., Flurpiridaz F-18 PET myocardial perfusion imaging in patients with suspected coronary artery disease, J. Am. Coll. Cardiol. 82 (16) (2023) 1598–1610.

[129] A.V Alashi .B., S. Thorn, S. Martins, Liang Guo, E. Moulton, X. Papademetris, R. Guzman, C. Mena, K. Smolderen, C. Liu, A.J. Sinusas, RB-82 positron emission tomography provides a reproducible assessment of regional lower extremity perfusion and perfusion reserve distinct from ankle brachial indices, in: 28th Annual Scientific Session of the American Society of Nuclear Cardiology; 2023; Toronto: Journal of Nuclear Cardiology, 2023.
[130] M.R. Stacy, M.W. Maxfield, A.J. Sinusas, Targeted molecular imaging of angiogenesis in PET and SPECT: a review, Yale J. Biol. Med. 85 (1) (2012) 75–86.
[131] M.R. Stacy, J.C. Paeng, A.J. Sinusas, The role of molecular imaging in the evaluation of myocardial and peripheral angiogenesis, Ann. Nucl. Med. 29 (3) (2015) 217–223.
[132] H. Leong-Poi, J. Christiansen, P. Heppner, C.W. Lewis, A.L. Klibanov, S. Kaul, et al., Assessment of endogenous and therapeutic arteriogenesis by contrast ultrasound molecular imaging of integrin expression, Circulation 111 (24) (2005) 3248–3254.
[133] J. Xie, Y. Liao, L. Yang, J. Wu, C. Liu, W. Xuan, et al., Ultrasound molecular imaging of angiogenesis induced by mutant forms of hypoxia-inducible factor-1alpha, Cardiovasc. Res. 92 (2) (2011) 256–266.
[134] J. Jo, X. Lin, T. Nakahara, I. Aoki, T. Saga, Y. Tabata, Preparation of polymer-based magnetic resonance imaging contrast agent to visualize therapeutic angiogenesis, Tissue Eng. Part A 19 (1–2) (2013) 30–39.
[135] J. Hua, L.W. Dobrucki, M.M. Sadeghi, J. Zhang, B.N. Bourke, P. Cavaliere, et al., Noninvasive imaging of angiogenesis with a 99mTc-labeled peptide targeted at alphavbeta3 integrin after murine hindlimb ischemia, Circulation 111 (24) (2005) 3255–3260.
[136] L.W. Dobrucki, D.P. Dione, L. Kalinowski, D. Dione, M. Mendizabal, J. Yu, et al., Serial noninvasive targeted imaging of peripheral angiogenesis: validation and application of a semiautomated quantitative approach, J. Nucl. Med. 50 (8) (2009) 1356–1363.
[137] I. Laitinen, A. Saraste, E. Weidl, T. Poethko, A.W. Weber, S.G. Nekolla, et al., Evaluation of alphavbeta3 integrin-targeted positron emission tomography tracer 18F-galacto-RGD for imaging of vascular inflammation in atherosclerotic mice, Circ. Cardiovasc. Imaging 2 (4) (2009) 331–338.
[138] M. Dietz, C.H. Kamani, E. Deshayes, V. Dunet, P. Mitsakis, G. Coukos, et al., Imaging angiogenesis in atherosclerosis in large arteries with (68)Ga-NODAGA-RGD PET/CT: relationship with clinical atherosclerotic cardiovascular disease, EJNMMI Res. 11 (1) (2021) 71.
[139] J.C. Ryu, B.P. Davidson, A. Xie, Y. Qi, D. Zha, J.T. Belcik, et al., Molecular imaging of the paracrine proangiogenic effects of progenitor cell therapy in limb ischemia, Circulation 127 (6) (2013) 710–719.
[140] Y. Tekabe, Q. Li, G. Zhang, J. Johnson, A.M. Schmidt, M. Backer, et al., Imaging VEGF receptors and alpha(v)beta(3) Integrins in a mouse Hindlimb ischemia model of peripheral arterial disease, Mol. Imaging Biol. 20 (6) (2018) 963–972.
[141] J.L. Goggi, A. Haslop, R. Boominathan, K. Chan, V. Soh, P. Cheng, et al., Imaging the proangiogenic effects of cardiovascular drugs in a diabetic model of limb ischemia, Contrast Media Mol. Imaging 2019 (2019) 2538909.
[142] H. Orbay, H. Hong, J.M. Koch, H.F. Valdovinos, T.A. Hacker, C.P. Theuer, et al., Pravastatin stimulates angiogenesis in a murine hindlimb ischemia model: a positron emission tomography imaging study with (64)Cu-NOTA-TRC105, Am. J. Transl. Res. 6 (1) (2013) 54–63.
[143] J.K. Willmann, K. Chen, H. Wang, R. Paulmurugan, M. Rollins, W. Cai, et al., Monitoring of the biological response to murine hindlimb ischemia with 64Cu-labeled vascular endothelial growth factor-121 positron emission tomography, Circulation 117 (7) (2008) 915–922.
[144] G. Hendrikx, S. Voo, M. Bauwens, M.J. Post, F.M. Mottaghy, SPECT and PET imaging of angiogenesis and arteriogenesis in pre-clinical models of myocardial ischemia and peripheral vascular disease, Eur. J. Nucl. Med. Mol. Imaging 43 (13) (2016) 2433–2447.
[145] M.R.Y.D. Stacy, M.W. Maxfield, Multimodal- ity imaging approach for serial assessment of regional changes in lower extremity arteriogenesis and tissue perfusion in a porcine model of peripheral arterial disease, Circ. Cardiovasc. Imaging 7 (1) (2014) 92–99.
[146] J. Hedhli, M. Kim, H.J. Knox, J.A. Cole, T. Huynh, M. Schuelke, et al., Imaging the landmarks of vascular recovery, Theranostics 10 (4) (2020) 1733–1745.
[147] C.Z. Behm, B.A. Kaufmann, C. Carr, M. Lankford, J.M. Sanders, C.E. Rose, et al., Molecular imaging of endothelial vascular cell adhesion molecule-1 expression and inflammatory cell recruitment during vasculogenesis and ischemia-mediated arteriogenesis, Circulation 117 (22) (2008) 2902–2911.
[148] D.J.W. Hulsen, C. Mitea, J.J. Arts, D. Loeffen, J. Geurts, Diagnostic value of hybrid FDG-PET/MR imaging of chronic osteomyelitis, Eur. J. Hybrid Imaging 6 (1) (2022) 15.
[149] T.H. Chou, M.R. Stacy, Clinical applications for radiotracer imaging of lower extremity peripheral arterial disease and critical limb ischemia, Mol. Imaging Biol. 22 (2) (2020) 245–255.
[150] X. Wang, Y.H. Nai, J. Gan, C.P.L. Lian, F.K. Ryan, F.S.L. Tan, et al., Multi-modality imaging of atheromatous plaques in peripheral arterial disease: integrating molecular and imaging markers, Int. J. Mol. Sci. 24 (13) (2023).
[151] M. Horger, S.M. Eschmann, C. Pfannenberg, D. Storek, R. Vonthein, C. D. Claussen, et al., Added value of SPECT/CT in patients suspected of having bone infection: preliminary results, Arch. Orthop. Trauma Surg. 127 (3) (2007) 211–221.
[152] S. Heiba, D. Kolker, L. Ong, S. Sharma, A. Travis, V. Teodorescu, et al., Dual-isotope SPECT/CT impact on hospitalized patients with suspected diabetic foot infection: saving limbs, lives, and resources, Nucl. Med. Commun. 34 (9) (2013) 877–884.
[153] E. Celiker-Guler, T.D. Ruddy, R.G. Wells, Acquisition, processing, and interpretation of PET (18)F-FDG viability and inflammation studies, Curr. Cardiol. Rep. 23 (9) (2021) 124.
[154] K.S. Myers, J.H. Rudd, E.P. Hailman, J.A. Bolognese, J. Burke, C.A. Pinto, et al., Correlation between arterial FDG uptake and biomarkers in peripheral artery disease, JACC Cardiovasc. Imaging 5 (1) (2012) 38–45.
[155] S.A. de Boer, M.C. Hovinga-de Boer, H.J. Heerspink, J.D. Lefrandt, A.M. van Roon, H.L. Lutgers, et al., Arterial stiffness is positively associated with 18F-fluorodeoxyglucose positron emission tomography-assessed subclinical vascular inflammation in people with early type 2 diabetes, Diabetes Care 39 (8) (2016) 1440–1447.
[156] X. Li, D. Heber, T. Leike, D. Beitzke, X. Lu, X. Zhang, et al., [68Ga]Pentixafor-PET/MRI for the detection of chemokine receptor 4 expression in atherosclerotic plaques, Eur. J. Nucl. Med. Mol. Imaging 45 (4) (2018) 558–566.
[157] O. Gaemperli, J. Shalhoub, D.R. Owen, F. Lamare, S. Johansson, N. Fouladi, et al., Imaging intraplaque inflammation in carotid atherosclerosis with 11C-PK11195 positron emission tomography/computed tomography, Eur. Heart J. 33 (15) (2012) 1902–1910.
[158] E. Gourni, O. Demmer, M. Schottelius, C. D'Alessandria, S. Schulz, I. Dijkgraaf, et al., PET of CXCR4 expression by a (68)Ga-labeled highly specific targeted contrast agent, J. Nucl. Med. 52 (11) (2011) 1803–1810.
[159] J.T. Thackeray, T. Derlin, A. Haghikia, L.C. Napp, Y. Wang, T.L. Ross, et al., Molecular imaging of the chemokine receptor CXCR4 after acute myocardial infarction, JACC Cardiovasc. Imaging 8 (12) (2015) 1417–1426.
[160] M. Reijrink, S.A. de Boer, C.A. Te Velde-Keyzer, J.K.E. Sluiter, R.A. Pol, H.J. L. Heerspink, et al., [(18)F]FDG and [(18)F]NaF as PET markers of systemic atherosclerosis progression: a longitudinal descriptive imaging study in patients with type 2 diabetes mellitus, J. Nucl. Cardiol. 29 (4) (2022) 1702–1709.
[161] M.M. Chowdhury, J.M. Tarkin, M.S. Albaghdadi, N.R. Evans, E.P.V. Le, T. B. Berrett, et al., Vascular positron emission tomography and restenosis in symptomatic peripheral arterial disease: a prospective clinical study, JACC Cardiovasc. Imaging 13 (4) (2020) 1008–1017.
[162] J. Ansari, F.N.E. Gavins, The impact of thrombo-inflammation on the cerebral microcirculation, Microcirculation 28 (3) (2021) e12689.
[163] B.L. Oliveira, F. Blasi, T.A. Rietz, N.J. Rotile, H. Day, P. Caravan, Multimodal molecular imaging reveals high target uptake and specificity of 111In- and 68Ga-labeled fibrin-binding probes for Thrombus detection in rats, J. Nucl. Med. 56 (10) (2015) 1587–1592.
[164] F. Blasi, B.L. Oliveira, T.A. Rietz, N.J. Rotile, H. Day, P.C. Naha, et al., Radiation dosimetry of the fibrin-binding probe (6)(4)cu-FBP8 and its feasibility for PET imaging of deep vein thrombosis and pulmonary embolism in rats, J. Nucl. Med. 56 (7) (2015) 1088–1093.
[165] R. Bing, M.A. Deutsch, S.L. Sellers, C.A. Corral, J.P.M. Andrews, E.J.R. van Beek, et al., 18F-GP1 positron emission tomography and bioprosthetic aortic valve thrombus, JACC Cardiovasc. Imaging 15 (6) (2022) 1107–1120.
[166] D. Izquierdo-Garcia, P. Desogere, A.L. Philip, C. Mekkaoui, R.B. Weiner, O. A. Catalano, et al., Detection and characterization of thrombosis in humans using fibrin-targeted positron emission tomography and magnetic resonance, JACC Cardiovasc. Imaging 15 (3) (2022) 504–515.
[167] B.L. Oliveira, P. Caravan, Peptide-based fibrin-targeting probes for thrombus imaging, Dalton Trans. 46 (42) (2017) 14488–14508.
[168] S.S. Segal, Regulation of blood flow in the microcirculation, Microcirculation 12 (1) (2005) 33–45.
[169] D.T. Kurjiaka, S.S. Segal, Interaction between conducted vasodilation and sympathetic nerve activation in arterioles of hamster striated muscle, Circ. Res. 76 (5) (1995) 885–891.
[170] M. Ohyanagi, J.E. Faber, K. Nishigaki, Differential activation of alpha 1- and alpha 2-adrenoceptors on microvascular smooth muscle during sympathetic nerve stimulation, Circ. Res. 68 (1) (1991) 232–244.
[171] J.A. Fallavollita, B.M. Heavey, A.J. Luisi Jr., S.M. Michalek, S. Baldwa, T. L. Mashtare Jr., et al., Regional myocardial sympathetic denervation predicts the risk of sudden cardiac arrest in ischemic cardiomyopathy, J. Am. Coll. Cardiol. 63 (2) (2014) 141–149.
[172] H. Khakpour, M. Vaseghi, Risk stratification and sudden cardiac death: is it time to include autonomic variables? Circ. Cardiovasc. Imaging 10 (8) (2017).
[173] K. Pacak, G. Eisenhofer, J.A. Carrasquillo, C.C. Chen, S.T. Li, D.S. Goldstein, 6-[18F]fluorodopamine positron emission tomographic (PET) scanning for diagnostic localization of pheochromocytoma, Hypertension 38 (1) (2001) 6–8.
[174] C.J. Tack, P.J. van Gurp, C. Holmes, D.S. Goldstein, Local sympathetic denervation in painful diabetic neuropathy, Diabetes 51 (12) (2002) 3545–3553.
[175] P. Magnusson, J. Nordstrom, H.J. Harms, M. Lubberink, F. Gadler, J. Sorensen, et al., Positron emission tomography ((15)O-water, (11)C-acetate, (11)C-HED) risk markers and nonsustained ventricular tachycardia in hypertrophic cardiomyopathy, Int. J. Cardiol. Heart Vasc. 26 (2020) 100452.
[176] A.J. Sinusas, J. Lazewatsky, J. Brunetti, G. Heller, A. Srivastava, Y.H. Liu, et al., Biodistribution and radiation dosimetry of LMI1195: first-in-human study of a novel 18F-labeled tracer for imaging myocardial innervation, J. Nucl. Med. 55 (9) (2014) 1445–1451.
[177] C. Franzius, K. Hermann, M. Weckesser, K. Kopka, K.U. Juergens, J. Vormoor, et al., Whole-body PET/CT with 11C-meta-hydroxyephedrine in tumors of the

sympathetic nervous system: feasibility study and comparison with 123I-MIBG SPECT/CT, J. Nucl. Med. 47 (10) (2006) 1635–1642.
[178] M. Yu, J. Bozek, M. Lamoy, M. Guaraldi, P. Silva, M. Kagan, et al., Evaluation of LMI1195, a novel 18F-labeled cardiac neuronal PET imaging agent, in cells and animal models, Circ. Cardiovasc. Imaging 4 (4) (2011) 435–443.
[179] M.R. Stacy, D.Y. Yu, M.W. Maxfield, I.M. Jaba, B.P. Jozwik, Z.W. Zhuang, et al., Multimodality imaging approach for serial assessment of regional changes in lower extremity arteriogenesis and tissue perfusion in a porcine model of peripheral arterial disease, Circ. Cardiovasc. Imaging 7 (1) (2014) 92–99.